An examination of the vapour-liquid interface of associating fluids using a SAFT-DFT approach

Felipe J. Blas [§,†], Elvira Martín del Río [§], Enrique de Miguel [§] and George Jackson [†,¶]

[§] *Departamento de Física Aplicada e Ingeniería Eléctrica, Escuela Politécnica Superior, Universidad de Huelva, 21819 La Rábida, Huelva, SPAIN*

[†] *Department of Chemical Engineering and Chemical Technology, Imperial College of Science, Technology and Medicine, Prince Consort Road, London SW7 2BY, UK*

[¶] Author to whom all correspondence should be addressed. E-mail: G.Jackson@ic.ac.uk

With a realistic description of the free energy of bulk fluids, it is now possible to make accurate predictions at the molecular level for the phase behaviour of systems as complex as aqueous solutions of amphiphiles, reacting and associating fluids, polymers, and electrolytes (e.g., using the statistical associating fluid theory SAFT). A quantitative molecular description of the interfacial properties of inhomogeneous fluids, including the surface tension and adsorption is much less common. In this work we first hope to improve the general understanding of the effect of association on the vapour-liquid interface. The vapour-liquid interface of the inhomogenous associating fluid is examined by combining the SAFT and density functional theory (DFT) approaches. A simple SAFT-HS representation is employed as it incorporates all of the essential physics of associating fluids and provides a good representation of the vapour pressure and coexisting phases. In this simplified SAFT approach the bulk fluid is represented as a hard-core reference, the association is treated with Wertheim's first order perturbation theory (TPT1), and a van der Waals mean-field approximation is used for the dispersive attractive interactions. In order to keep the representation of the bulk fluid and interface at the same level of approximation we use the van der Waals theory for non-uniform fluids, which is a DFT at the level of a local density approximation (LDA); the correlations are neglected in the attractive non-local term. The vapour-liquid interface of model systems with one, two and four bonding sites are examined for varying degrees of association. As expected, a stronger site-site interaction is generally found to sharpen the interface (decrease the interfacial thickness) and increase the surface tension. In the case of a dimerising (single site) fluid a limiting behaviour is reached for full association (saturation) where the molecular species are dimers. After an in depth analysis of the effect of association on the vapour-liquid interface, we highlight the strengths of our simple SAFT-DFT approach by making some quantitative comparisons with experimental surface tensions for selected systems including water and replacement refrigerants.

1 Introduction

A great deal of effort has been spent in recent years on the development and use of accurate equations of state for the determination of the thermodynamic properties and phase equilibria of fluid systems (see Ref. [1] for a recent review). With a realistic description of the free energy of bulk fluids, it is now possible to make quantitative predictions at the molecular level for the phase behaviour of systems as complex as aqueous solutions of amphiphiles, reacting and associating fluids, polymers, and electrolytes. An accurate molecular description of the interfacial properties of inhomogeneous fluids, including the surface tension and adsorption is much less common. Processes which occur at surfaces are central to most aspects of our daily lives: the nature of the interfaces between the lipid bilayers that form cell membranes and the aqueous environment inside and outside the cell are very sensitive to the presence of solutes and other molecular species, especially in the case of surface active agent (surfactants); the stability of colloids (emulsions such as milk or areosols such as smoke) are profoundly affected by surface effects; the formation of micelles and lyotropic liquid crystalline phases formed by amphiphilic surfactant molecules in aqueous solution (soaps, cosmetics, foodstuffs, etc.) is governed by a delicate interplay between surface and bulk contributions to the free energy; a description of adsorption at solid surfaces is also of prime importance in understanding the processes involved in catalytic reactions and corrosion. These few examples clearly indicate the importance of inhomogenous systems, as well as the desirability of developing an accurate predictive theory of surface phenomena.

The most successful modern theory of inhomogeneous classical fluids is undeniably the density functional method, in which the free energy of the system is expressed as a functional of the spacially varying single particle density. An excellent account of density functional theory (DFT) is given in the review by Evans [2]; in this brief introduction we will focus only on the salient features that relate to our work. Onsager [3, 4] was one of the first to use a 'density' functional approach in his treatment of the isotropic-

nematic transition in a system of infinitely long rods; here, the free energy is written as a functional of the singlet orientational distribution function (single particle 'density') at the crude level of the second virial coefficient. In historical terms, Onsager's seminal paper appears to have been overlooked until the renewed interest in anisotropic phase transitions of hard body models during the 1980s. The density functional method owes much of its origins to the description of the inhomogeneous quantum electron fluid. In the mid 1970s it became apparent that the approaches developed a decade earlier for the electron fluid could be readily applied in the area of classical fluids to yield a number of useful approximate schemes, including the square gradient approximation or the type of perturbation theory that we employ in the current work [5, 6, 7]. The first calculation of the density profile and surface tension of the vapour-liquid interface of a Lennard-Jones fluid using a perturbation theory about a hard-sphere reference is due to Toxvaerd [8]; in this pioneering work he employed the local density approximation (LDA) for the repulsive reference fluid and used a mean density to evaluate the correlation function of the inhomogeneous reference fluid. If the correlations are ignored completely in the perturbation term the approach simplifies to the so-called 'van der Waals theory' of non-uniform fluids; the reader is referred to the paper by Sullivan [9] for a detailed discussion of this approximation. As short-range correlations in the fluid are also neglected in the LDA approach the theory can not be used to describe oscillatory density profiles of the type exhibited by confined fluids. Although the van der Waals treatment may appear to be a rather drastic approximation, this simple theory has been applied to numerous problems in interfacial phenomena and has provided great insight into the nature of the vapour-liquid interface, adsorption and wetting phenomena, and phase transitions in confined fluids [10, 11, 12]. An advantage of the van der Waals approximation is that one can sometimes invert the Ornstein-Zernike integral equation to obtain approximations for the inhomogeneous pair distribution functions, which are particularly useful in studies of phase transitions and wetting [13, 14]. In this work we hope to provide a clear example

of how a simple van der Waals like DFT can be used successfully to describe the vapour-liquid interface of complex associating fluids such as water. No description of DFT, however brief, would be complete without a mention of weighted-density approximations [15, 16, 17, 18, 19, 20, 21, 22, 23, 24, 25]. Most schemes that have been proposed to improve the van der Waals free energy functional focus on a more accurate treatment of the reference system, which is described at the local density level, instead of the inclusion of correlations in the mean-field treatment of the long-range attractive interactions. The idea of a weighted-density approximation (WDA) is that an appropriate average of the density over a local volume is used to describe the residual reference free energy instead of the local density. The advantage of using a WDA is that one can reproduce the oscillatory profiles found for a fluid close to a solid boundary. In a wonderful example of the broad applicability of DFT to the three principal states of matter, Curtin and Ashcroft [26] used a WDA to accurately describe the vapour-liquid and solid-liquid phase boundaries together with the triple point of the Lennard-Jones system. Although a WDA will generally give the best description of the inhomogeneous system, in studies of the vapour-liquid interface a free energy functional treated at the LDA level is often found to give a good description of the interfacial properties.

The thermodynamic and structural properties of the inhomogeneous system such as the density profiles, interfacial tensions, the solvation forces, and phase transitions are prescribed by the precise form of the free energy functional. The difficulty with DFT is that accurate free energies are known for only a small number of systems. In practice this has meant that DFT studies of interfacial phenomena have been largely limited to well defined models and few direct comparisons with experiment have been made. In contrast, the past decades has seen the development of highly accurate equations of states for the bulk thermodynamic properties of complex fluid mixtures: one of the most sophisticated, successful, and versatile has been the statistical associating fluid theory (SAFT) [27, 28] and its many extensions (see the recent review by Müller and Gubbins [29]). In the

SAFT approach the separate contributions of molecular length (non-sphericity), inter- and intra-molecular association (hydrogen bonding) and dispersion (attractive) forces are described as separate perturbation terms in the free energy; the molecules are modelled as chains of attractive spherical segments with short-range bonding sites which mediate the molecular association. The origins of the approach lie in the theory of Wertheim [30] where associating molecules are treated in the context of both a perturbation theory and an integral equation. The perturbation expressions of Wertheim were initially incorporated into an equation of state for mixtures of associating chain molecules formed from hard-sphere segments, with the dispersion forces treated at the mean-field level of van der Waals [31, 32]; this prototype of the SAFT equation of state, more recently referred to as SAFT-HS [33], is essentially an augmented van der Waals equation, and is used here as the basis of a van der Waals-like DFT for inhomogeous associating fluids. SAFT was originally formulated to describe chains formed from Lennard-Jones segments with the structure of the hard-sphere fluid as a reference [27, 28], although an accurate description of the monomer Lennard-Jones reference fluid has also been employed [34, 35, 36, 37, 38, 39, 40, 41, 42, 43]. In more more recent versions of the theory, the approach has been extended to deal with associating chain molecules formed from attractive segments of variable range (SAFT-VR) by using a second-order high-temperature perturbation expansion [44, 45]. The use of the SAFT-VR approach in studies of fluid phase equilibria provides a good example of the accuracy of the SAFT free energy in describing the bulk thermodynamics of systems ranging from small strongly associating molecules such as water [46] and replacement refrigerants [47], to long-chain alkanes [48] and polymers [49], and electrolyte solutions [46, 50]. Numerous examples of the use of SAFT in the description of the phase equilibria of complex fluids and mixtures can be found in the extensive correlations of Huang and Radosz [51, 52] and in the review by Müller and Gubbins [29].

Before we discuss the application of DFT for inhomogeneous associating fluids within

the context of the Wertheim and SAFT approaches, it is important to acknowledge the use of the alternative model of association introduced by Cummings and Stell [53, 54, 55]. Studies of inhomogenous systems of associating spherical molecules adsorbed (or desorbed) on different types of surfaces with singlet and pair integral equations are too numerous to describe in detail [56]. The molecule-molecule and molecule-surface association are found to have a profound effect on the density profiles describing the adsorption of the molecules. The application of DFT is generally simpler and computationally less demanding than approaches based on integral equation theories. The use of Wertheim's perturbation theory for association within a DFT approach was first suggested by Chapman [57]. Such an approach has been used with a WDA to study associating fluids of hard spherical molecules with bonding sites (similar to the models that we use in this study) confined between hard walls, and good agreement with simulation is obtained [58, 59, 60, 61]. The same type of DFT has been used by Sokołowski and co-workers to study associating fluids between planar walls and in pores [62]. Of particular interest here are related DFT studies of the vapour-liquid interface of a dimerising Lennard-Jones fluid [63], of the effect of confinment on the vapour-liquid density profiles [64], and of gas-liquid nucleation in dimerising fluids [65]. The theory of Wertheim has also been applied to study 'polymeric' fluids consisting of fully associated hard-sphere chains using a DFT approach with the Kierlik and Rosinberg WDA [66, 67, 68, 69, 70]; in this case the Henderson-Abraham-Barker integral equation theory [71] gives a better overall description of system than the DFT.

There have also been some more phenomenological thermodynamic studies of inhomogeneous associating fluids. Suresh and co-workers [72] have examined association at a liquid-solid interface using a monolayer lattice-type theory, and have compared their results with the density functional theory of Segura *et al.* [59]. A square-gradient Cahn-Hillard description with a crude treatment of the partition function for hydrogen bond formation has been used to study the interfacial properties of water [73]; in this case the

focus was on the anomolous behaviour in the supercooled region. The SAFT approach has also been implemented within the Cahn-Hillard theory to describe the vapour-liquid surface tension of alkanes, alcohols, and water in terms of an empirical adjustable parameter [74]; although the SAFT description offered the best representation of the interfacial properties for the group of equations of state studied, this approach did not give accurate surface tensions, especially near the critical point. An interfacial equation of state has been developed using SAFT and the mean-spherical approximation (MSA) to describe systems involving aqueous solutions of surfactant with and without added salt [75]; considering the complexity of these systems the approach provides a good representation of the interfacial tension, but again this is at the expense of using an empirical adjustable parameter. The limited predictive capabilities of these empirical approaches restrict the applicability of such methods to cases where something is known about the interfacial properties of the system under investigation. DFT approaches, although more difficult to apply to systems that are of practical interest, are truly molecular, and offer a predictive platform for inhomogeneous systems not only for interfacial properties such as the surface tension and excess surface adsorption but also for density profiles and the thickness of the interface.

Two main points have probably become clear from the ensuing discussion. The first is that the overwhelming majority of integral equation and DFT studies of inhomogeneous associating systems have focused on the solid-fluid interface and confined systems. There is great need for studies of the vapour-liquid interface of associating systems. The second point is that the systems examined in most of these studies are highly idealised models such as associating hard-sphere and Lennard-Jones molecules. This has meant that there has been little or no contact between the DFT studies and experiment. Often, however, the step between an idealised and a realistic description is not a large one: in the case of water, for example, a hard-sphere spherical core with four square-well bonding sites and with the dispersion attractive interactions treated at the mean-field level provides a

good description of the bulk vapour-liquid equilibria [33]. In our current paper we first hope to improve the general understanding of the effect of association on the vapour-liquid interface by examining model systems with one, two and four bonding sites. The SAFT description of the free energy of the associating fluid is used as it provides a good description of the bulk associating fluid. The inhomogenous vapour-liquid interface of the associating fluid will be examined by combining the SAFT and DFT approaches. This represents one of a series of papers in which we examine the vapour-liquid, and liquid-liquid interface of systems with increasing complexity; our final goal is to make quantitative predictions of the surface tension and surface excess adsorption of systems comprising water, oil, and surfactant. We start with the simplest SAFT-HS representation that incorporates all of the essential physics of associating fluids and provides a good representation of the vapour pressure and coexisting densities of strongly associated fluids such as water [33]: in this simplified SAFT approach the bulk fluid is represented as a hard-sphere reference, the association is treated with the Wertheim first order perturbation theory (TPT1), and the dispersive attractive interactions are treated with a van der Waals mean-field term. In order to keep the representation of the bulk fluid and interface at the same level of approximation we use the van der Waals theory for nonuniform fluids which, as mentioned earlier, is a DFT at the LDA level. The advantages of using such a simple van der Waals DFT are that the extension to mixtures is straighforward, that the theory can be improved by incorporating correlations in the nonlocal term or by examining WDAs, and that the resulting Euler-Lagrange equation is relatively easy to solve by iteration. The main drawback of such a theory is that the mean-field form of direct correlation function does not include the short-range correlations and oscillatory density profiles, which are especially significant in representing confined systems. In the case of the vapour-liquid interface, however, the density profile is a smoothly varying function of position, and a van der Waals treatment is generally adequate. After an in depth analysis of the effect of association on the vapour-liquid interface for a number of

model systems, we will highlight the strengths of our simple SAFT-DFT approach by making some quantitative comparisons with experimental surface tensions for water and some replacement refrigerants.

2 Model and theory

In this work we consider associating fluids in which molecules are formed from tangent spheres (monomers) each of diameter σ. The interaction between monomers has two contributions: a short-range repulsive part, given by a hard-sphere potential, and a long-range attractive term, modelled as a Yukawa potential,

$$\phi_Y(r) = -\epsilon \, \frac{\exp\left[-\lambda(r/\sigma - 1)\right]}{(r/\sigma)}, \tag{1}$$

where r is the distance between the centres of the monomers, ϵ is the depth of the potential, and λ^{-1} is the range of the attractive interactions. This choice of the dispersive term is particularly suited for the description of screened polar interactions the most common of which are the Coulombic interactions found in electrolytes and colloids, as well as in aqueous systems. The precise form of the attractive interaction is not important in this study, and a Lennard-Jones or square-well potential can also be used [76].

Association between the molecules is mediated by one (or more) embedded off-centre bonding sites (see figure 1) placed at a distance r_d from the centre of a given monomer. The site-site interaction is represented by a square-well potential of range r_c and depth ϵ^{hb}.

This model, although rather crude, accounts for the most salient features of real associating chain molecules, such as bead connectivity (representing topological constraints and internal flexibility), excluded volume effects, attractive forces between molecules, and highly anisotropic short-range attractive interactions that characterise hydrogen-bonding. This type of model is at the heart of the SAFT modeling of fluids [29].

As was discussed in the introduction, density functional theory constitutes the most convenient route for a theoretical analysis of the interfacial properties of fluids. For convenience, we consider an open system at temperature T and chemical potential μ in a volume V. In the absence of external fields, the grand potential Ω of the inhomogeneous system is given by [2, 12]

$$\Omega[\rho(\boldsymbol{r})] = F[\rho(\boldsymbol{r})] - \mu \int d\boldsymbol{r}\rho(\boldsymbol{r}), \tag{2}$$

where $\rho(\boldsymbol{r})$ is the number density at position $\boldsymbol{r}$, and $F[\rho(\boldsymbol{r})]$ is the intrinsic Helmholtz free energy of the system, which is a functional of $\rho(\boldsymbol{r})$. Following a perturbative scheme, it will be assumed that $F[\rho(\boldsymbol{r})]$ can be expressed as [2, 12]

$$F[\rho(\boldsymbol{r})] = \int d\boldsymbol{r} f^{ref}(\boldsymbol{r}) + F^{att}[\rho(\boldsymbol{r})], \tag{3}$$

where the first term on the right-hand side (reference term) accounts for the relevant contributions of the intermolecular interactions (repulsive forces, short-range association and chain contribution) to the free energy; F^{att} is the contribution to the free energy due to the dispersive attractive interactions.

It will be assumed that the reference term can be treated in a local density approximation (LDA) such that $f^{ref}(\boldsymbol{r}) = f^{ref}(\rho(\boldsymbol{r}))$ is the Helmholtz free energy density of a (spatially) uniform system with constant density $\rho(\boldsymbol{r})$ [2, 12].

Following the usual perturbation DFT, the attractive contribution can be written as [2, 12]

$$F^{att}[\rho(\boldsymbol{r})] = \frac{1}{2} \int d\boldsymbol{r}\, d\boldsymbol{r}' \rho(\boldsymbol{r})\rho(\boldsymbol{r}')g^{ref}(\boldsymbol{r}, \boldsymbol{r}')\phi^{att}\left(|\boldsymbol{r} - \boldsymbol{r}'|\right). \tag{4}$$

In the mean-field description the correlations between molecules at $\boldsymbol{r}$ and $\boldsymbol{r}'$ are neglected ($g^{ref}(\boldsymbol{r}, \boldsymbol{r}') = 1$) and the free energy is given by [2, 12]

$$F^{att}[\rho(\boldsymbol{r})] = \frac{1}{2}\int d\boldsymbol{r}\, d\boldsymbol{r'}\rho(\boldsymbol{r})\rho(\boldsymbol{r'})\phi^{att}\left(|\boldsymbol{r}-\boldsymbol{r'}|\right), \tag{5}$$

where $\phi^{att}\left(|\boldsymbol{r}-\boldsymbol{r'}|\right)$ is the attractive part of the intermolecular potential between the segments that form the chains.

In the spirit of the bulk SAFT-HS equation of state [31, 32, 33], we propose the following expression for $f^{ref}(\rho(\boldsymbol{r}))$:

$$f^{ref}(\rho(\boldsymbol{r})) = f^{ideal}(\rho(\boldsymbol{r})) + f^{hs}(\rho(\boldsymbol{r})) + f^{chain}(\rho(\boldsymbol{r})) + f^{assoc}(\rho(\boldsymbol{r})). \tag{6}$$

This free energy reference function is essentially the LDA version of the Chapman DFT [58, 59, 60, 61]. In equation (6), f^{ideal} is the ideal gas contribution:

$$f^{ideal}(\rho(\boldsymbol{r})) = k_B T\rho(\boldsymbol{r})\left[\ln\left(\Lambda^3\rho(\boldsymbol{r})\right) - 1\right], \tag{7}$$

where k_B is the Boltzmann constant, and Λ the thermal de Broglie wavelength. f^{hs} is the (residual) free energy density of a fluid of hard spheres, represented here by the Carnahan-Starling expression [77, 78]:

$$f^{hs}(\rho(\boldsymbol{r})) = k_B T\rho(\boldsymbol{r})\frac{4\eta(\boldsymbol{r}) - 3\eta^2(\boldsymbol{r})}{(1-\eta(\boldsymbol{r}))^2}, \tag{8}$$

where $\eta = (\pi/6)\rho\sigma^3 = b\rho$ is the packing fraction and b is the segment volume. f^{chain} is the Helmholtz free energy density due to the formation of the chain molecule [79, 31, 32],

$$f^{chain}(\rho(\boldsymbol{r})) = -k_B T\rho(\boldsymbol{r})(m-1)\ln g^{hs}(\sigma;\rho(\boldsymbol{r})), \tag{9}$$

where m is the number of segments per molecule; $g^{hs}(\sigma;\rho(\boldsymbol{r}))$ is the contact value of the monomer-monomer hard-sphere pair radial distribution function, given by the expression of Carnahan and Starling [77, 78],

$$g^{hs}(\sigma;\rho(\boldsymbol{r})) = \frac{1-\eta(\boldsymbol{r})/2}{(1-\eta(\boldsymbol{r}))^3}. \tag{10}$$

The association contribution in equation (6), f^{assoc}, is obtained directly from Wertheim's first-order thermodynamic perturbation theory [30] in terms of $X_A(\boldsymbol{r})$, the fraction of molecules located at $\boldsymbol{r}$ not bonded at a given site A:

$$f^{assoc}(\rho(\boldsymbol{r})) = k_B T \rho(\boldsymbol{r}) \left\{ \sum_A \left(\ln X_A(\boldsymbol{r}) - \frac{X_A(\boldsymbol{r})}{2} \right) + \frac{1}{2} n \right\}, \tag{11}$$

where n is the number of associating sites. As Chapman [57], and Kierlik and Rosinberg [66, 67, 68] note, the theory of Wertheim is formulated in the context of inhomogeneous fluids. At the first-order level, equation (11) is exact even in a more general non-local context. In Wertheim's formalism, $X_A(\boldsymbol{r})$ is given by a set of coupled mass-action equations [30]:

$$X_A(\boldsymbol{r}) = \left\{ 1 + \sum_B \int d\boldsymbol{r}' \rho(\boldsymbol{r}') X_B(\boldsymbol{r}') \Delta_{AB}(\boldsymbol{r}') \right\}^{-1}. \tag{12}$$

The term Δ_{AB} in the integrand can be approximated by [31, 32]:

$$\Delta_{AB} = K_{AB} F_{AB} g^{hs}(\sigma;\rho(\boldsymbol{r})), \tag{13}$$

where K_{AB} is the volume available for bonding sites A and B, $F_{AB} = \exp(\epsilon^{hb}/k_B T) - 1$, ϵ^{hb} is the site-site association energy. The volume available for bonding sites A and B is simply given by [31, 32],

$$K_{AB} = \frac{4\pi\sigma^3}{72 r_d^{*2}} \Big[\ln(r_c^* + 2r_d^*)(6r_c^{*3} + 18 r_c^{*2} r_d^* - 24 r_d^{*3}) +$$

$$(r_c^* + 2r_d^* - 1)(22 r_d^{*2} - 5 r_c^* r_d^* - 7 r_d^* - 8 r_c^{*2} + r_c^* + 1) \Big], \tag{14}$$

where $r_d^* = r_d/\sigma$ and $r_c^* = r_c/\sigma$ are the reduced distance from the centre of the hard sphere

to the centre of the association site and the reduced square-well range, respectively.

At equilibrium $\Omega[\rho(\boldsymbol{r})]$ is a minimum and the corresponding density profile $\rho(\boldsymbol{r})$ is obtained by a minimisation with respect to $\rho(\boldsymbol{r})$:

$$\frac{\delta\Omega[\rho(\boldsymbol{r})]}{\delta\rho(\boldsymbol{r})} = 0. \tag{15}$$

Since we are dealing with planar vapour-liquid interfaces, the density profile is only a function of z, the position along the direction perpendicular to the interface. This allows us to write the Euler-Lagrange equation (15) as

$$k_B T \left\{ \frac{\partial f^{ideal}(\rho(z))}{\partial\rho(z)} + \frac{\partial f^{hs}(\rho(z))}{\partial\rho(z)} + \frac{\partial f^{chain}(\rho(z))}{\partial\rho(z)} + \frac{\partial f^{assoc}(\rho(z))}{\partial\rho(z)} \right\} +$$

$$\int_{-\infty}^{+\infty} dz' \rho(z') \overline{\phi}^{att}(|z - z'|) - \mu = 0 \tag{16}$$

In this equation $\overline{\phi}^{att}$ is obtained as an average over the radial and angular variables using cylindrical coordinates. The integrated attractive potential used in this work, which corresponds to segments that interact through the Yukawa intermolecular potential, is given by

$$\overline{\phi}_Y^{att}(|z - z'|) = \begin{cases} -\dfrac{2\pi}{\lambda}\epsilon & \text{if } |z - z'| \leq \sigma \\ -\dfrac{2\pi}{\lambda}\epsilon \exp\left[-\lambda\left(\dfrac{|z - z'|}{\sigma} - 1\right)\right] & \text{if } |z - z'| \geq \sigma \end{cases} \tag{17}$$

We follow the method used by Tjipto-Margo *et al.* [80] to solve the integral equation (16) numerically, since it has proved much more accurate than other simpler techniques [81, 82]. Equation (16) is solved over a grid of points between z_{min} and z_{max}, which are chosen so that $\rho(z)$ tends to the bulk liquid and vapour densities as $z \to z_{min}$ and $z \to z_{max}$, respectively.

Once the equilibrium density profile is obtained, the surface tension is calculated from the simple thermodynamic identity [2, 12],

$$\gamma = \frac{\Omega + PV}{A}. \tag{18}$$

where A is the area of the interface and P the bulk pressure.

The width of the interface (w) is defined as the distance over which the density changes from $\rho_V^{bulk} + 0.1(\rho_L^{bulk} - \rho_V^{bulk})$ to $\rho_V^{bulk} + 0.9(\rho_L^{bulk} - \rho_V^{bulk})$, where ρ_L^{bulk} and ρ_V^{bulk} are the liquid and vapour coexistence densities, respectively.

To determine the interfacial properties at a given temperature, accurate values of bulk properties (densities, pressure, and chemical potential) of the coexisting phases are required. These values are obtained from the Helmholtz free energy functional given by equation (3) which, in the limit of a uniform system $\rho(z) = \rho^{bulk}$, reduces to the SAFT-HS free energy [31, 32]. The mean-field treatment of the attractive term F^{att} in our DFT is consistent with the use of a van der Waals-like attractive free energy in the SAFT-HS approach [31, 32],

$$F^{att} = -N_s \eta \epsilon^{mf}, \tag{19}$$

where $N_s = mN$ is the number of segments of the system and ϵ^{mf} is an integrated van der Waals mean-field energy. At the mean-field level of approximation of the SAFT-HS approach, the particular form used for the attractive potential is irrelevant. However, this is no longer the case with a non-uniform fluid, and a specific intermolecular attractive interaction must be considered [2, 12]. Since the functional given by equation (3) has to reduce to the SAFT-HS Helmholtz free energy in the bulk limit, the dispersive energy parameter of the attractive potential must satisfy the following relation:

$$2\pi \int_\sigma^\infty \phi^{att}(r) r^2 dr = -\frac{\pi}{6}\sigma^3 \epsilon^{mf} = -b\epsilon^{mf}. \tag{20}$$

The dispersive energy associated with the attractive part of the intermolecular potential is related to the value of ϵ^{mf} by equation (20). Depending on the form of the attractive

potential chosen to represent the fluid in a given application, a different relation between the attractive potential parameters and the integrated van der Waals energy must be used.

3 Results and discussion

We apply the SAFT-DFT approach outlined in the previous section to study the vapour-liquid interface for two types of systems: i) fluids of associating spherical molecules, and ii) fluids of non-associating chain molecules. We first consider systems of spherical molecules, with one or two association sites, and investigate the effect of association on interfacial properties, such as the surface tension, the interfacial thickness, and the distribution of associated clusters through the vapour-liquid interface. Systems of non-associating chain molecules are then considered to investigate the influence of chain length or molecular shape on the surface tension. We also briefly discuss the effect of the range of the dispersive interactions on the interfacial properties. The predictions for the surface tension for simple models of water and replacement refrigerants are also compared with experimental values in order to assess the adequacy of our SAFT-DFT approach.

Before studying the interfacial behaviour of the associating fluids, we use the bulk SAFT-HS equation of state to determine the vapour-liquid equilibrium by solving the equilibrium conditions:

$$p_L(\eta_L, T) = p_V(\eta_V, T) \tag{21}$$

$$\mu_L(\eta_L, T) = \mu_V(\eta_V, T) \tag{22}$$

where the subscripts refer to the liquid (L) and vapour (V) phases. In the following discussion, the integrated mean-field energy ϵ^{mf} is chosen as the unit of energy and the hard-sphere diameter σ as the unit of length. According to this, we define the following re-

duced quantities: temperature, $T^* = k_B T/\epsilon^{mf}$; pressure, $P^* = Pb/\epsilon^{mf}$; bonding volume, $K^* = K/\sigma^3$; strength of the site-site association interaction, $\epsilon^{hb*} = \epsilon^{hb}/\epsilon^{mf}$; interfacial thickness, $w^* = w/\sigma$; and surface tension $\gamma^* = \gamma\sigma^2/\epsilon^{mf}$.

3.1 Spherical associating molecules

The interfacial properties for fluids consisting of spherical associating molecules can be obtained from equations (2)-(5) by neglecting the chain contribution, $f^{chain} = 0$. Molecules with either one or two bonding sites are considered for different values of the association energy, ϵ^{hb*}. In all cases, the associating sites are characterised by a bonding volume $K^* = 5.55938 \times 10^{-4}$, which corresponds to the choice $r_d^* = 0.25$ and a range of $r_c^* = 0.55$ for the site-site association potential defined in section 2.

We first consider the case in which the molecules have a single site A with a site-site energy of $\epsilon^{hb*} = 1$. Only A-A bonding is allowed so that only dimerisation is possible. The density profiles, $\rho(z)$, at different temperatures for a fixed range of the Yukawa potential corresponding to $\lambda = 1.5$ are shown in figure 2. These profiles exhibit the expected behaviour: at low temperatures the curves represent a sharp interface, which corresponds to a high value of the surface tension, and as the temperature increases towards the critical value ($T_c^* = 0.116270$), the profiles become broader.

The effect of association through the interface is examined by calculating the fraction of molecules not bonded (monomers); the appropriate interfacial profile is shown in figure 3a for a reduced temperature of $T^* = 0.070$, which is well below the critical point. At this temperature, dimerisation occurs to different extent in the liquid and vapour phases. The degree of dimerisation is greater in the liquid than in the vapour because of the difference in density [31, 32]: about 95% of the molecules are bonded in the bulk liquid phase ($X_A \sim 0.05$) and about 40% are bonded in the bulk vapour phase ($X_A \sim 0.6$). It is interesting to note that the profile for the fraction of monomers is shifted towards the gas phase with respect to the vapour-liquid interface: this means that the fraction

of monomers saturate to a constant value in the liquid phase before the density profile reaches the bulk limit ρ_L^{bulk}, while the fraction of monomers is still increasing to the bulk vapour limit even when the vapour density has saturated to its constant bulk value ρ_V^{bulk}. This effect was also observed with a Wertheim DFT and Monte Carlo simulation for a one-site associating Lennard-Jones fluid by Borówko *et al.* [63].

The behaviour of the interfacial profile for the fraction of monomers has also been studied at a higher temperature of $T^* = 0.105$, which is very close to the critical point. As shown in figure 3b, the fraction of monomers increases in both the vapour and liquid phases when the temperature is increased: about 70% of the molecules are bonded in the bulk liquid ($X_A \sim 0.3$) and about 30% are bonded in the bulk vapour ($X_A \sim 0.7$). This is due to the strong effect of the temperature on X_A, which dominates the effect of the density [31, 32]. As for the lower temperatures, the profile for the fraction of monomers is shifted towards the vapour side of the interface with respect to the density profile.

In figure 4 we present the temperature dependence of the surface tension for systems of spherical molecules with one bonding site for different values of the association energy; for comparison the limiting cases of no association ($\epsilon^{hb*} = 0$) and complete dimerisation ($\epsilon^{hb*} = \infty$) are also included. The surface tension of associating systems at a fixed temperature increases for larger values of the association energy. This effect, which is related to a larger cohesive energy in the system as the value of ϵ^{hb*} is increased, is consistent with the sharper density profiles found at lower temperatures (see figure 2). At low temperatures there is a near linear dependence of the surface tension with temperature, with a stronger curvature close to the critical point. A noticeable effect of strong association is the large change in the slope of the surface tension curves compared to that of a non-associating system. At a given temperature, the slope of the surface tension curves becomes more negative as ϵ^{hb*} is increased; for large values of the association energy the slope decreases again and approaches the limiting value of complete dimerisation ($\epsilon^{hb*} = \infty$). A similar effect has also been observed for the vapour pressure of the same system (see figures 12

and 13 of Ref. [31]).

The effect of varying the degree of association on the interfacial thickness is also considered for the same values of the site-site energy (see figure 5). The main consequence of more association is to decrease the thickness of the interface at fixed temperature, which is consistent with a larger cohesive energy. This behaviour is in contrast to that reported by Borówko *et al.* [63] for a dimerising Lennard-Jones in which there appears to be little or no effect of association on the interfacial thickness; the poor characterisation of the density profiles and relatively small samples which were examined could be responsible for this inconsistency.

To summarise the results for a dimerising fluid, the main effect of molecular association is to increase the surface tension and decrease the interfacial thickness, with a corresponding shift of the curves to higher temperatures due to the larger critical point.

We next proceed to investigate the vapour-liquid interface of fluids of spherical molecules with two anisotropic bonding sites (see figure 1b). In this case, the two bonding sites, denoted by A and B, are only allowed to form AB bonds (no AA or BB association is considered). The range of the Yukawa potential ($\lambda = 1.5$) and the bonding volume ($K^* = 5.55938 \times 10^{-4}$) are taken to be the same as for the one-site system, and the effect of association on the interfacial behaviour is again studied for several values of the bonding energy ϵ^{hb*}.

When a molecule has two associating sites, chain aggregates can form. Although the theory presented here does not yield direct information on the distribution of clusters, the fraction of clusters of a given size can be estimated using purely statistical arguments (see Ref. [31] for further details). We have calculated the fraction of molecules not bonded at sites A and B along the liquid-vapour interface, and hence obtain the average aggregate size, $m(z)$, as the inverse of the fraction $X_A(z)$ (or $X_B(z)$) using the relation [31, 32]

$$m(z) = X_A^{-1}(z) = X_B^{-1}(z). \tag{23}$$

Initially, we consider the two-site spherical molecules with a site-site energy of $\epsilon^{hb*} = 1$. The average aggregate size across the interfacial region is shown in figure 6 for different temperatures. At a temperature of $T^* = 0.097$, which is well below the critical temperature ($T_c^* = 0.129429$), the average aggregate size is close to 7 in the bulk liquid, and the vapour phase is mainly monomeric. These results indicate that the liquid phase consists mainly of large aggregates, while the vapour phase consists almost entirely of unassociated molecules. As the temperature is raised towards the critical point, the average aggregate size in the liquid phase rapidly decreases. The opposite behaviour is found in the vapour phase (but to a lesser extent), where an increase in temperature results in the formation of slightly larger aggregates. Close to the critical point, the liquid and vapour phases have similar densities, and hence, the average aggregate size tends to the same constant value.

The temperature dependence of the surface tension and the interfacial thickness of spherical molecules with two association sites for different bonding energies are presented in figures 7 and 8. For comparison, we also include the results for the non-associating ($\epsilon^{hb*} = 0$) limit. As can be seen from figure 7, the surface tension again increases as the association energy increases. The surface tension curves are also seen to shift towards higher temperatures for the larger degree of association.

A change of curvature in the surface tension curves is observed for the two-site systems, an effect which was not found in the case of molecules with a single bonding site. This effect can be ascribed to the existence of large clusters in the fluid, particularly for the highly associated systems. In the case of the one-site fluid (see figure 4) the limiting coexistence curve of the fully dimerised system (hard dumbbell) is approached as the bonding energy is increased. By contrast, the two-site system is not limited to dimer formation, and the surface tension curves are shifted to increasingly higher temperatures as the association energy increases.

The surface tension, when plotted *versus* the temperature, shows a *convex* curvature at intermediate temperatures, while for non-associating and one-site systems, a *concave*

curvature is always observed. As can be seen from figure 7, this effect is more pronounced as the association energy is increased. The behaviour predicted by the SAFT-DFT equations is consistent with the available experimental data for the surface tension of strongly associating fluids, such as water and some replacement refrigerants, as will be shown in the final section.

The results for the interfacial thickness of the two-site systems are displayed in figure 8. At a given temperature the interface becomes sharper as the association energy is increased. This is compatible with the behaviour found for the surface tension (cf figure 7).

In summary, the main effect of association on the interfacial properties of fluids of spherical molecules with two associating sites is a shift of the surface tension curves to higher temperatures as the degree of association is increased. A similar conclusion was made in the case of the one-site system, but with an important difference: the curves are bounded by the limit of full dimerisation ($\epsilon^{hb*} \to \infty$) in the case of molecules with a single site whereas for molecules with two sites systems with aggregates of increasing length are obtained.

3.2 Non-associating chain molecules

The Helmholtz free energy functional for non-associating fluids of homonuclear hard-sphere chains can be obtained from equations (2)-(5) by neglecting the contribution due to association, $f^{assoc} = 0$.

The temperature dependence of the surface tension for non-associating fluids consisting of chain-like molecules formed from m spherical segments (see figure 1 c)) is shown in figure 9. An increase in the chain length of the molecules has two major effects on the surface tension. Firstly, the critical temperature of the fluid increases, and there is a corresponding shift of the surface tension curves to higher temperatures. Secondly, the surface tension increases as the chain length of the molecules becomes larger; this effect

is expected as the cohesive energy of the system becomes larger as the molecules become longer.

It is gratifying to find that the relatively simple SAFT-DFT approach presented here yields the correct qualitative trends for the dependence of the surface tension with chain lengths observed experimentally for systems such as the n-alkanes. In the final section we will present a preliminary comparison with experiment for selected systems.

3.3 Effect of the range of the mean-field dispersion term

Before direct comparisons are made for real systems, we briefly discuss the effect of the range of the dispersive attractive interactions (in this particular case the Yukawa potential) on the interfacial properties. This has been studied in more detail for the Yukawa and square-well models in another publication [76]. The range of the dispersion forces turns out to be a useful parameter in the quantitative description of the surface tension of real systems.

In our mean-field SAFT-HS treatment of the vapour-liquid equilibria the range and strength of the dispersive interactions are coupled in such a way that the integrated dispersive energy (van der Waals attractive constant) remains constant (see equation (20)). At this van der Waals level the bulk vapour-liquid equilibria (vapour-pressure, coexisting densities etc.) is unique for a given value of the van der Waals integrated constant regardless of the specific values of the range and depth of the potential. This is not however true for the interfacial properties which are sensitive to the precise form of the potential. We exemplify this by examining a non-associating Yukawa fluid at the mean-field SAFT-DFT level for various ranges of the attractive interaction, but keeping the integrated dispersive energy constant.

The temperature dependence of the surface tension for a Yukawa fluid is shown in figure 10 for different ranges of the attractive interaction. As expected the surface tension is seen to increase with increasing range; there is a corresponding increase in the slope of

the surface tension curve. This effect is due to an increase in the overall cohesive energy of molecules associated with the interface. It is clear from the figure, that the range of the potential can be adjusted to provide the appropriate slope of the surface tension curve, a feature which we take advantage of in making comparisons with real systems.

3.4 Preliminary comparison with experiment

The models of the type described in the previous sections have been widely used to examine the phase equilibria of a wide variety of real systems, including n-alkanes, carboxylic acids, alcohols, water, and other strongly associating systems, such as hydrogen fluoride and replacement refrigerants (see the detailed review in Ref. [1]). The interfacial properties of strongly associated systems present features which are markedly different from those exhibited by non-associating systems. For example, the surface tension-temperature curve for water has a characteristic s-shape, corresponding to regions with negative (far from the critical region) and positive (in the critical region) curvature, while the surface tension of the n-alkanes decreases monotonically with increasing temperature ([83]).

We now use the SAFT-DFT developed in the previous sections to examine the interfacial properties (particularly the surface tension) of water and two refrigerants, difluoroethane (HFC-32) and 1,1,1,2-tetrafluoroethane (HFC-134a). As in earlier work [33], the water molecule is modelled as a hard-spherical repulsive core of diameter σ with four embedded off-centre square-well bonding sites to mediate the hydrogen bonding (see figure 1d). The four bonding sites account for the two electron lone pairs and the two hydrogen sites of the water molecule. The sites are placed in a tetrahedral geometry, although the relative locations of the bonding sites are not taken into account within the first-order approximation of the theory used here. The dispersive attractive interactions between water molecules are represented by a Yukawa potential (eq. (1)), treated at the mean-field level of approximation. The values of the molecular size (σ), integrated mean-field attractive energy (ϵ^{mf}), hydrogen-bond energy (ϵ^{hb}), and bonding volume (K), are taken

from previous work [33], and are presented in table 1. This set of parameters represents the best fit to the vapour pressures and saturated liquid densities of water from the triple to the critical point, rescaled to reproduce the critical point.

The refrigerants HFC-32 and HFC-134a are both polar molecules, but it is not clear whether or not they form hydrogen bonds. Recent neutron scattering experiments for trifluoromethane (HFC-24) suggest that these types of molecules do not hydrogen bond [84]. As in previous work the models used to represent the refrigerants do not include an explicit contribution for the polar interactions, but include two bonding sites in order to account for the dipolar anisotropy of the molecules; accordingly, the attractive interaction due to the dipoles, or weak hydrogen bonds, are treated as a type of association [47, 85]. The HFC-32 refrigerant is modelled as a single hard sphere, and HFC-134a as two fused hard spheres with $m = 1.35$; the non-sphericity parameter is chosen so as to give the best agreement with the experimental vapour-liquid equilibrium data. The remaining intermolcular parameters are taken from Ref. [85] and are summarised in table 1.

A preliminary comparison of the SAFT-DFT predictions with the experimental values of the surface tension of water [86] is shown in figure 11. As can be seen, the agreement between experimental data and the theoretical results is excellent over the whole range of temperatures. The range parameter $\lambda \sim 2$ provides the best description of the surface tension curve. It is very pleasing to note that SAFT-DFT is able to reproduce the s-shaped curve with a change in curvature from *concave* to *convex* of water. This characteristic is not exhibited by non-associating fluids and can be ascribed to hydrogen bonding.

The SAFT-DFT predictions for the temperature dependence of the surface tension of HFC-32 and HFC-134a are shown in figures 12 and 13, respectively. The theoretical description of the surface tension of HFC-32 (figure 11) are again found to be in excellent agreement with experiment [87] for a range parameter of $\lambda \sim 1$. In the case of HFC-134a, the agreement between experimental data and theory is equally good for a similar value of $\lambda \sim 1.5$.

4 Conclusions

In this paper we have focussed on the effect of association on the vapour-liquid interfacial properties of pure fluids using a SAFT based density functional theory (DFT). The theory is essentially a van der Waals (mean-field) theory of non-uniform fluids with the reference term treated within the local density approximation (LDA). The main effect of association is found to be sharpen the vapour-liquid interface and to increase the surface tension. In the case of molecules with one bonding site, the behaviour is bounded between the non-associating and completely dimerised limits. By contrast, an increase in association for the two-site molecules leads to aggregates of increasing length and the surface tension curves are shifted to increasingly higher temperatures. By taking the limit of complete association the SAFT-DFT theory can be used to represent chain molecules of a fixed chain length. Since the theory presented here is based on a LDA, smooth density profiles are expected and this approach can not be used to describe very high inhomogeneities. In particular, certain interfacial effects associated to the solid-liquid phase transition could only be observed when a non-local approach is used.

This preliminary and relatively simple SAFT-DFT is found to provide a good description of the surface tension of strongly associating molecules such as water and replacement refrigerants. In future work we plan to improve the treatment of the interfacial properties by using a perturbation theory such as SAFT-VR [44] to describe the bulk phases, rather than the crude mean-field description used in the current work. A more sophisticated treatment such as that of Kierlik and Rosinberg [66, 67] will also be used to describe chain molecules; in the current work all of the segments making up the chain are treated in an equivalent local fashion so that all information about the orientation of molecule at the interface is lost. One of our final goals is to examine the interfaces of mixtures including aqueous solutions of surfactants using a molecular based SAFT-DFT of the type described in this paper.

Acknowledgement

F.J.B. would like to thank BP Amoco Exploration and the Oil Extraction programme of the Engineering and Physical Sciences Research Council (EPSRC) for a research fellowship (GR/N20317). We acknowledge support from the Joint Research Equipment Initiative (JREI) of the EPSRC for computer hardware (GR/M94427), and the Royal Society-Wolfson Foundation for the award of a refurbishment grant. This work was also supported by a research project from VII Plan Propio de Investigación de la Universidad de Huelva. This financial support is gratefully acknowledged.

References

[1] SENGERS, J. V., KAYSER, R. F., PETERS, C. J., and WHITE, H. J. Jr (eds.), 2000, *Equations of State for Fluids and Fluid Mixtures* (Amsterdam: Elsevier).

[2] EVANS, R., 1992, *Fundamentals of Inhomogeneous Fluids*, edited by D. Henderson (New York: Marcel Dekker).

[3] ONSAGER, L., 1942, *Phys. Rev.*, **62**, 558.

[4] ONSAGER, L., 1949, *Ann. N. Y. Acad. Sci.*, **51**, 627.

[5] EBNER, C., SAAM, W. F., and STROUD, D., 1976, *Phys. Rev. A*, **14**, 2264.

[6] SAAM, W. F., and EBNER, C., 1977, *Phys. Rev. A.*, **15**, 2566.

[7] YANG, A. J. M., FLEMING, P. D., and GIBBS, J. H., 1976, *J. Chem. Phys.*, **64**, 3732.

[8] TOXVAERD, S., 1971, *J. Chem. Phys.*, **55**, 3116.

[9] SULLIVAN, D. E., 1982, *Phys. Rev. A*, **25**, 1669.

[10] SULLIVAN, D. E., and TELO DA GAMA, M. M., 1986, *Fluid Interfacial Phenomena*, edited by C. A. Croxton (New York: Wiley).

[11] DIETRICH, S., 1988, *Phase Transitions and Critical Phenomena*, edited by C. Domb and J. L. Lebowitz (New York: Academic Press).

[12] EVANS, R., 1990, *J. Phys.: Condens. Matter*, **2**, 8989.

[13] TARAZONA, P., and EVANS, R., 1982, *Molec. Phys.*, **47**, 1033.

[14] PARRY, A. O., and EVANS, R., 1989, *J. Phys.: Condens. Matter*, **1**, 7202.

[15] NORDHOLM, S., JOHNSON, M., and FREASIER, B. C., 1980, *Aust. J. Chem.*, **33**, 2139.

[16] JOHNSON, M., and NORDHOLM, S., 1981, *J. Chem. Phys.*, **75**, 1953.

[17] ROBLEDO, A., and VAREA, C., 1981, *J. Stat. Phys.*, **26**, 513.

[18] PERCUS, J. K., 1982, *J. Stat. Phys.*, **28**, 67.

[19] TARAZONA, P., 1984, *Molec. Phys.*, **52**, 81.

[20] TARAZONA, P., and EVANS, R., 1984, *Molec. Phys.*, **52**, 847.

[21] TARAZONA, P., 1985, *Phys. Rev. A*, **31**, 2672; Erratum, 1985, *Phys. Rev. A*, **32**, 3148.

[22] CURTIN, W. A., and ASHCROFT, N. W., 1985, *Phys. Rev. A*, **32**, 2909.

[23] GROOT, R. D., and VAN DE EERDEN, J. P., 1987, *Phys. Rev. A*, **36**, 4356.

[24] ROSENFELD, Y., 1989, *Phys. Rev. Lett.*, **63**, 980.

[25] KIERLIK, E., and ROSINBERG, M. L., 1990, *Phys. Rev. A*, **42**, 3382.

[26] CURTIN, W. A., and ASHCROFT, N. W., 1986, *Phys. Rev. Lett.*, **56**, 2775.

[27] CHAPMAN, W. G., GUBBINS, K. E., JACKSON G., and RADOSZ, M., 1989, *Fluid Phase Equilib.*, **52**, 31.

[28] CHAPMAN, W. G., GUBBINS, K. E., JACKSON, G., and RADOSZ, M., 1990, *Ind. eng. Chem. Res.*, **29**, 1709.

[29] MÜLLER, E. A., and GUBBINS, K. E., 2000, *Associating Fluids and Fluid Mixtures*, edited by J. V. Sengers, R. F. Kayser, C. J. Peters, and H. J. White (Amsterdam: Elsevier).

[30] WERTHEIM, M. S., 1984, *J. Stat. Phys.*, **35**, 19; *Ibid.*, **35**, 35; 1986, *Ibid.*, **42**, 459; 1986, *Ibid.*, **42**, 477.

[31] JACKSON, G., CHAPMAN, W. G., and GUBBINS, K. E., 1988, *Molec. Phys.*, **65**, 1.

[32] CHAPMAN, W. G., JACKSON, G., and GUBBINS, K. E., 1988, *Molec. Phys.*, **65**, 1057.

[33] GALINDO, A., WHITEHEAD, P. J., JACKSON, G., and BURGESS, A. N., 1996, *J. Phys. Chem.*, **100**, 6781.

[34] CHAPMAN, W. G., 1990, *J. Chem. Phys.*, **93**, 4299.

[35] JOHNSON, J. K., and GUBBINS, K. E., 1992, *Molec. Phys.*, **77**, 1033.

[36] GHONASGI, D., and CHAPMAN, W. G., 1993, *Molec. Phys.*, **80**, 161.

[37] GHONASGI, D., LLANO-RESTREPO, M., and CHAPMAN, W. G., 1993, *J. Chem. Phys.*, **98**, 5662.

[38] GHONASGI, D., and CHAPMAN, W. G., 1994, *AIChE J.*, **40**, 878.

[39] JOHNSON, J. K., MÜLLER, E. A., and GUBBINS, K. E., 1998, *J. Phys. Chem.*, **98**, 6413.

[40] BLAS, F. J., and VEGA, L. F., 1997, *Molec. Phys.*, **92**, 135.

[41] BLAS, F. J., and VEGA, L. F., 1998, *Ind. eng. Chem. Res.*, **37**, 660.

[42] BLAS, F. J., and VEGA, L. F., 1998, *J. Chem. Phys.*, **109**, 7405.

[43] VEGA, L. F., and BLAS, F. J., 2000, *Fluid Phase Equil.*, **171**, 91.

[44] GIL-VILLEGAS, A., GALINDO, A., WHITEHEAD, P. J., MILLS, S. J., JACKSON, G., and BURGESS, A. N., 1997, *J. Chem. Phys.*, **104**, 4168.

[45] GALINDO, A., DAVIES, L. A., GIL-VILLEGAS, A., and JACKSON, G., 1998, *Molec. Phys.*, **93**, 241.

[46] GALINDO, A., GIL-VILLEGAS, A., JACKSON, G., and BURGESS, A. N., 1999, *J. Phys. Chem. B*, **103**, 10272.

[47] GALINDO, A., GIL-VILLEGAS, A., WHITEHEAD, P. J., and JACKSON, G., 1998, *J. Phys. Chem. B*, **102**, 7632.

[48] McCABE, C., and JACKSON G., 1999, *Phys. Chem. Chem. Phys.*, **1**, 2057.

[49] McCABE, C., GALINDO, A., GARCIA-LISBONA, M. N., and JACKSON, G., 2001, submitted.

[50] GIL-VILLEGAS, A., GALINDO, A., and JACKSON, G., 2001, *Molec. Phys.*, **99**, 531.

[51] HUANG, S. H., and RADOSZ, M., 1990, *Ind. eng. Chem. Res.*, **29**, 2284.

[52] HUANG, S. H., and RADOSZ, M., 1991, *Ind. eng. Chem. Res.*, **30**, 1994.

[53] CUMMINGS, P. T., and STELL, G., 1984, *Molec. Phys.*, **51**, 253; 1985, *Ibid.*, **55**, 33; 1987, *Ibid.*, **60**, 1315.

[54] STELL, G., and ZHOU, Y., 1989, *J. Chem. Phys.*, **91**, 3618; 1992, *Ibid.*, **96**, 1504.

[55] KALYUZHNYI, Yu. V., STELL, G., LLANO-RESTREPO, M. L., CHAPMAN, W. G., and HOLOVKO, M. F., 1994, *J. Chem. Phys.*, **101**, 7939.

[56] PIZIO, O., HENDERSON, D., and SOKOŁOWSKI, S., 1995, *J. Phys. Chem.*, **99**, 2408; TROKHYMCHUCK, A., PIZIO, O., HOLOVKO, M., and SOKOŁOWSKI, S., 1997, *J. Chem. Phys.*, **106**, 200; DUDA, Yu. Ja., SEGURA, C. J., VAKARIN, E., HOLOVKO, M. F., and CHAPMAN, W. G., 1998, *J. Chem. Phys.*, **108**, 9168.

[57] CHAPMAN, W. G. Chapman, 1988, PhD Thesis, 'Theory and Simulation of Associating Liquids', Cornell University.

[58] SEGURA, C. J., and CHAPMAN, W. G., 1995, *Molec. Phys.*, **86**, 415.

[59] SEGURA, C. J., CHAPMAN, W. G., and SHUKLA, K. P., 1997, *Molec. Phys.*, **90**, 759.

[60] SEGURA, C. J., CHAPMAN, W. G., VAKARIN, E., and HOLOVKO, M., 1998, *J. Chem. Phys.*, **108**, 4837.

[61] SEGURA, C. J., ZHANG, J., and CHAPMAN, W. G., 2001, *Molec. Phys.*, **99**, 1.

[62] PATRYKIEJEW, A., SOKOŁOWSKI, S., and HENDERSON, D., 1998, *Molec. Phys.*, **95**, 211; PATRYKIEJEW, A., and SOKOŁOWSKI, S., 1999, *J. Phys. Chem. B*, **103**, 4466; HUERTA, A., PIZIO, O., and SOKOŁOWSKI, S., 2000, *J. Chem. Phys.*, **112**, 4286.

[63] BORÓWKO, M., STEPNIAK, K., SOKOŁOWSKI, S., and ZAGORSKI, R., 1999, *Czech J. Phys.*, **49**, 1067.

[64] PIZIO, O., PATRYKIEJEW, A., and SOKOŁOWSKI, S., 2000, *J. Chem. Phys.*, **113**, 10761.

[65] TALANQUER, V., and OXTOBY, D. W., 2000, *J. Chem. Phys.*, **112**, 851.

[66] KIERLIK, E., and ROSINBERG, M. L., 1992, *J. Chem. Phys.*, **97**, 9222.

[67] KIERLIK, E., and ROSINBERG, M. L., 1993, *J. Chem. Phys.*, **99**, 3950.

[68] PHAN, S., KIERLIK, E., ROSINBERG, M. L., YETHIRAJ, A., and DICKMAN, R., 1995, *J. Chem. Phys.*, **102**, 2141.

[69] KIERLIK, E., PHAN, S., and ROSINBERG, M. L., 1996, *Am. Chem. Soc. Symp. Ser.*, Vol. **629**, 212.

[70] PIZIO, O., PATRYKIEJEW, A., and SOKOŁOWSKI, S., 2001, *Molec. Phys.*, **99**, 57.

[71] HOLOVKO, M. F., and VAKARIN, E. V., 1996, *Molec. Phys.*, **87**, 1375.

[72] SURESH, S. J., and NAIK, V. M., 1996, *Langmuir*, **12**, 6151; SURESH, S. J., and NAIK, V. M., 1997, *Langmuir*, **13**, 4785; SURESH, S. J., and NAIK, V. M., 1998, *J. Chem. Phys.*, **109**, 6021; SURESH, S. J., MISHRA, M., and PATNI, C., 1999, *J. Colloid Int. Sci.*, **210**, 225.

[73] MÜHLBACHER, L., 1998, *J. Chem. Phys.*, **108**, 10205.

[74] KAHL, H., and ENDERS, S., 2000, *Fluid Phase Equil.*, **172**, 27.

[75] FU, D., LU, J. F., BAO, T. Z., and LI, Y. G., 2000, *Ind. Eng. Chem. Res.*, **39**, 320.

[76] GLOOR, G. J., BLAS, F. J., MARTÍN DEL RIO, E., DE MIGUEL, E., and JACKSON, G., 2001, *Fluid Phase Equil.*, submitted.

[77] CARNAHAN, N. F., and STARLING, K. E., 1969, *J. Chem. Phys.*, **51**, 635.

[78] HANSEN, J. P., and McDONALD, I. R., 1986, *Theory of simple liquids* (London: Academic Press).

[79] WERTHEIM, M. S., 1986, *J. Chem. Phys.*, **85**, 2929.

[80] TJIPTO-MARGO, B., SEN, A. K., MEDEROS, L., and SULLIVAN, D. E., 1989, *Molec. Phys.*, **67**, 601.

[81] TELO DA GAMA, M. M., 1984, *Molec. Phys.*, **52**, 585.

[82] THURTELL, J. M., TELO DA GAMA, M. M., and GUBBINS, K. E., 1985, *Molec. Phys.*, **54**, 321.

[83] ROWLINSON, J. S., and WIDOM, B., 1982, *Molecular Theory of Capillarity* (Oxford: Oxford University Press).

[84] MORT, K. A., JOHNSON, K. A., COOPER, D. L., BURGESS, A. N., and HOWELLS, W. S., 1997, *Molec. Phys.*, **90**, 415.

[85] GALINDO, A., WHITEHEAD, P. J., JACKSON, G., and BURGESS, A. N., 1997, *J. Phys. Chem. B*, **101**, 2082.

[86] WAGNER, W., and KRUSE, A., 1997, *Properties of Water and Steam* (Spinger).

[87] *Physical Properties Data, KLEA*, ICI Chemicals and Polymers Ltd., 1993.

Table 1. Optimised parameters for the models of water (H_2O), difluoromethane (HFC-32), and 1,1,1,2-tetrafluoromethane (HFC-134a) taken from Ref. [33, 85].

Substance	m	σ/Å	(ϵ/k_B)/K	$(\epsilon^{hb}/\mathrm{k}_B)$/K	K/Å
H_2O	1	3.589	4384	1534	1.3499
HFC-32	1	3.705	2207	1426	5.2028
HFC-134a	1.35	4.020	2373	1487	4.2162

List of figures

critical temperature.

Figure 5. Interfacial thickness of spherical molecules with one associating site as a function of temperature for different values of the association energy. The curves represent the same values as in figure 4.

Figure 6. Average aggregate size across the vapour-liquid interface of spherical molecules with two associating sites at different temperatures: $T^* = 0.097$ (continuous curve), 0.104 (dotted curve), 0.110 (dashed curve), 0.116 (long-dashed curve), and 0.123 (dot-dashed curve). In all cases $K^* = 5.55938 \times 10^{-4}$ and $\epsilon^{hb*} = 1$.

Figure 7. Surface tension of spherical molecules with two associating sites as a function of temperature for different association energies: $\epsilon^{hb*} = 0$ (continuous curve), 1 (dotted curve), 2 (dashed curve), 3 (long-dashed curve), and 5 (dot-dashed curve). In all cases $K^* = 5.55938 \times 10^{-4}$. The inset also shows the dependence of the surface tension with the temperature reduced with respect to the critical temperature.

Figure 8. Interfacial thickness of spherical molecules with two associating sites as a function of temperature for different values of the association energy. The curves represent the same values as in figure 7.

Figure 9. Surface tension of non-associating chain molecules as a function of temperature. The curves are labelled according to the chain length m. The inset also shows the dependence of the surface tension with the temperature reduced with respect to the critical temperature.

Figure 10. Surface tension of non-associating spherical molecules as a function of temperature for Yukawa systems with different potential ranges: $\lambda^{-1} = 0.33$ (continuous curve), $\lambda^{-1} = 0.4$ (dotted curve), $\lambda^{-1} = 0.5$ (dashed curve), $\lambda^{-1} = 0.67$ (long-dashed

curve), and $\lambda^{-1} = 1$ (dot-dashed curve).

Figure 11. Surface tension as a function of temperature for water. The circles correspond to experimental data [86]; the curve represents the theoretical prediction using the SAFT-DFT approach with a set of parameters taken from Ref. [33] and $\lambda = 2$.

Figure 12. Surface tension as a function of temperature for HFC-32 (difluoromethane). The circles correspond to experimental data [87]; the curve represents the theoretical prediction using the SAFT-DFT approach with a set of parameters taken from Ref. [85] and $\lambda = 1$.

Figure 13. Surface tension as a function of temperature for HFC-134a (1,1,1,2-tetrafluoroethane). The circles correspond to experimental data; the curve represents the theoretical prediction using the SAFT-DFT approach with a set of parameters taken from [85] and $\lambda = 1.5$.

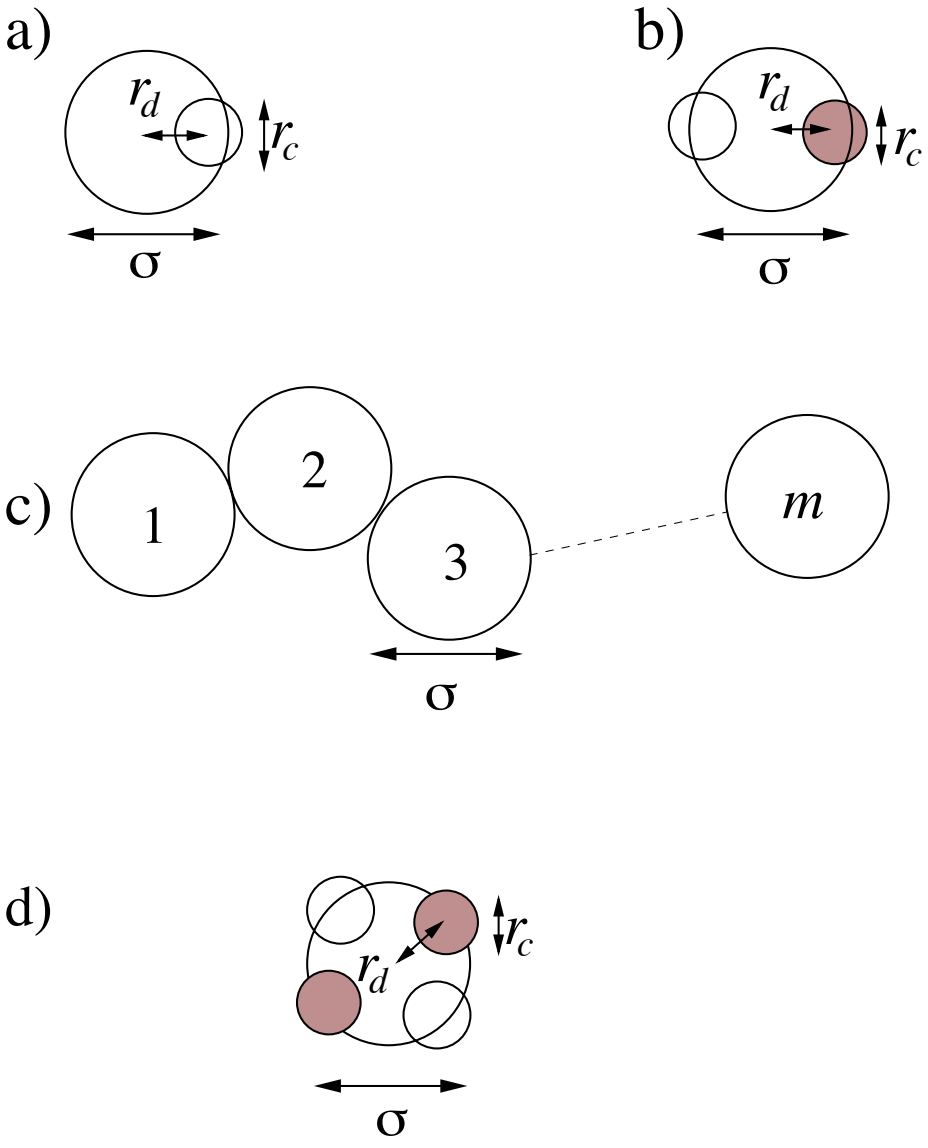
a)
r_d
r_c
σ
b)
r_d
r_c
σ
c)
1
2
3
m
σ
d)
r_d
r_c
σ

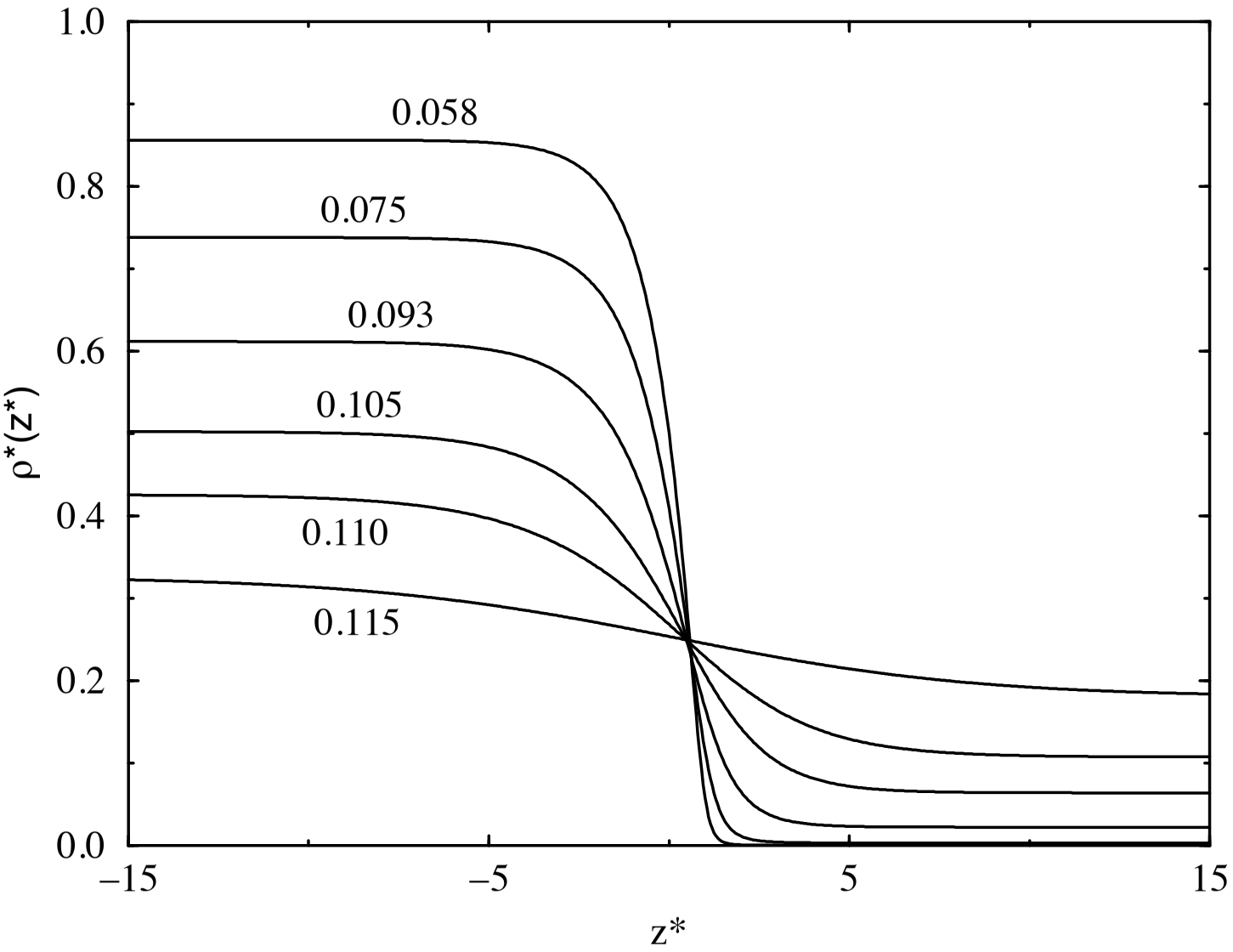
1.0
0.8
0.6
0.4
0.2
0.0
ρ*(z*)
0.058
0.075
0.093
0.105
0.110
0.115
−15
−5
5
15
z*

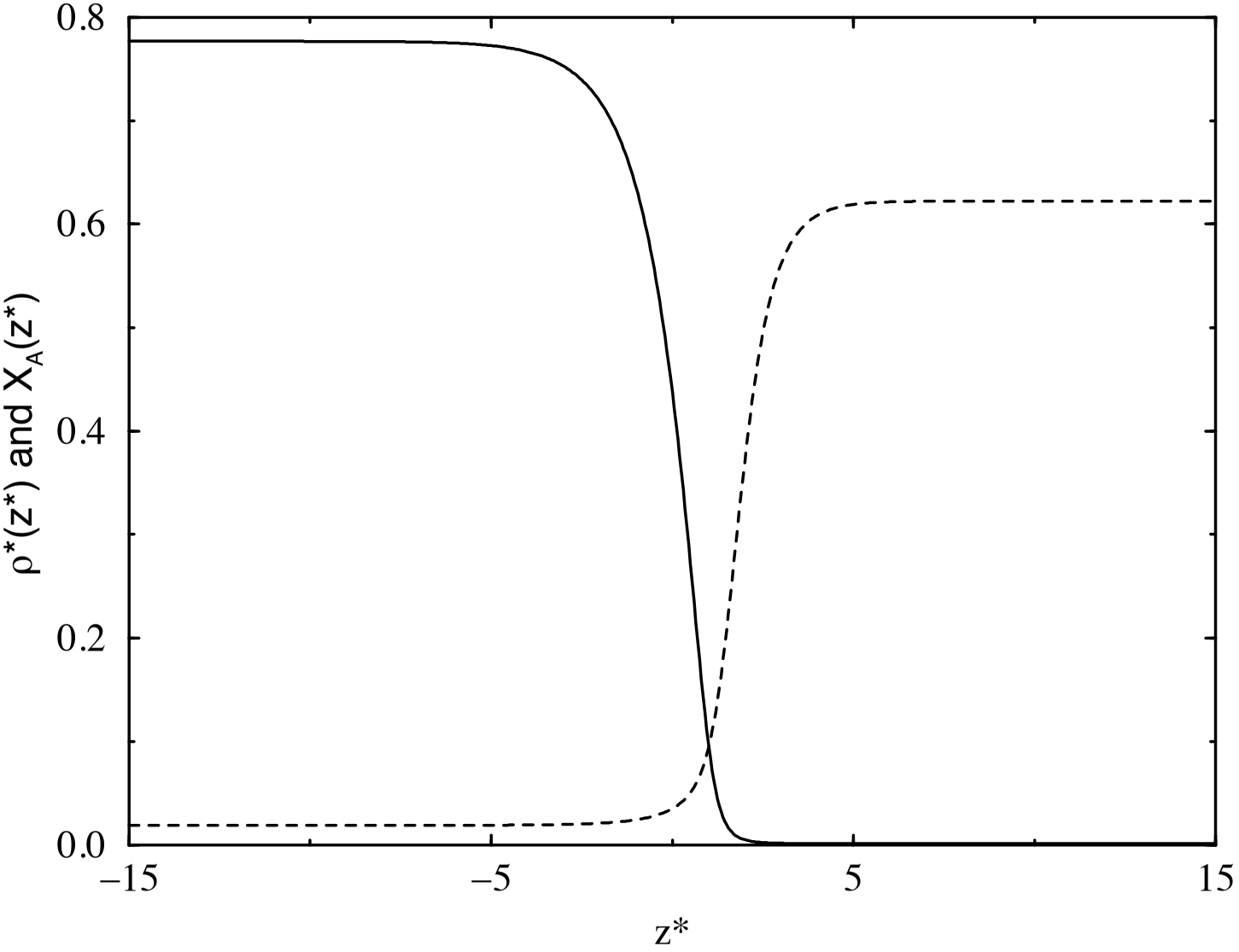
0.8
0.6
0.4
0.2
0.0
ρ*(z*) and X_A(z*)
–15
–5
5
15
z*

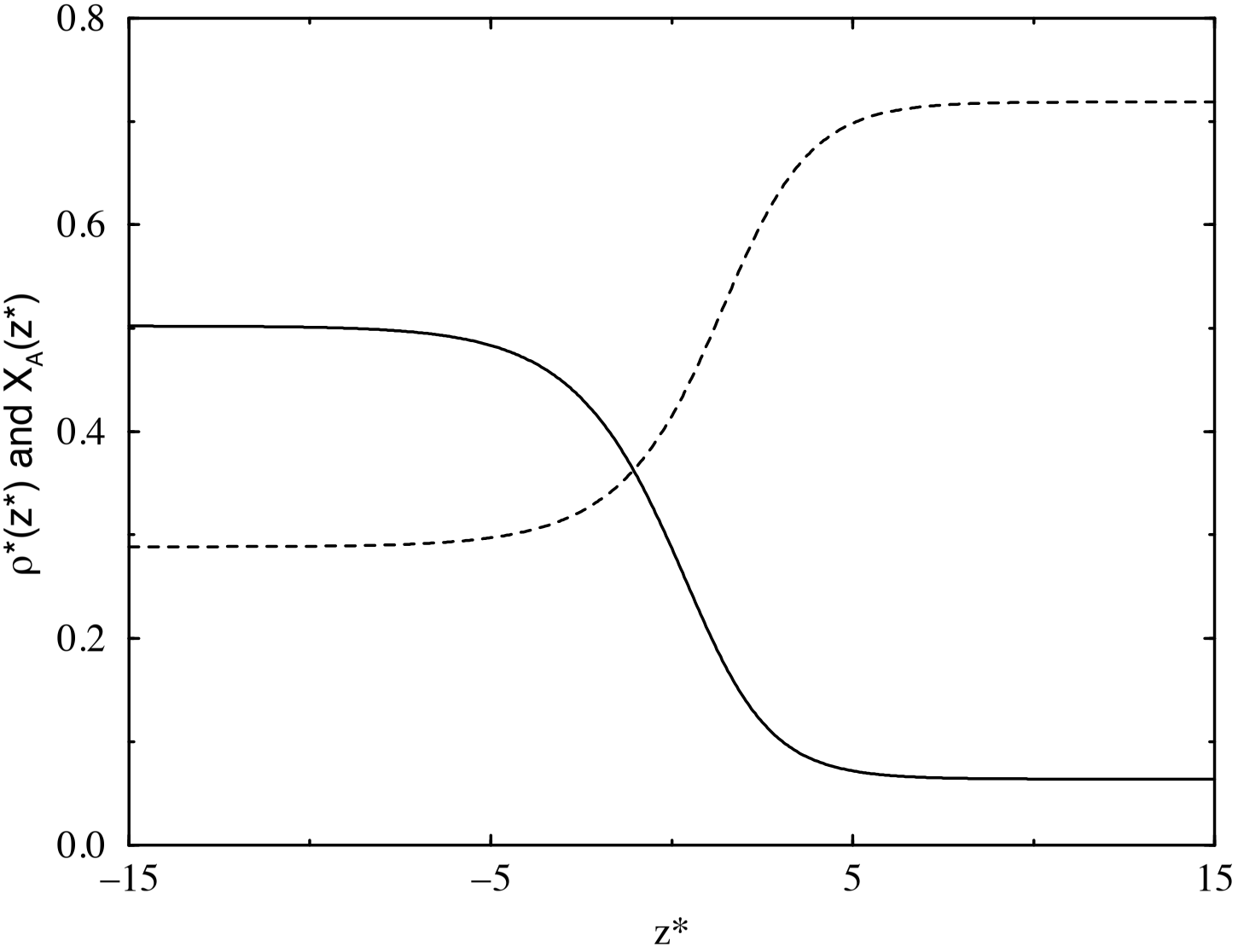
0.8
0.6
0.4
0.2
0.0
ρ*(z*) and X_A(z*)
−15
−5
5
15
z*

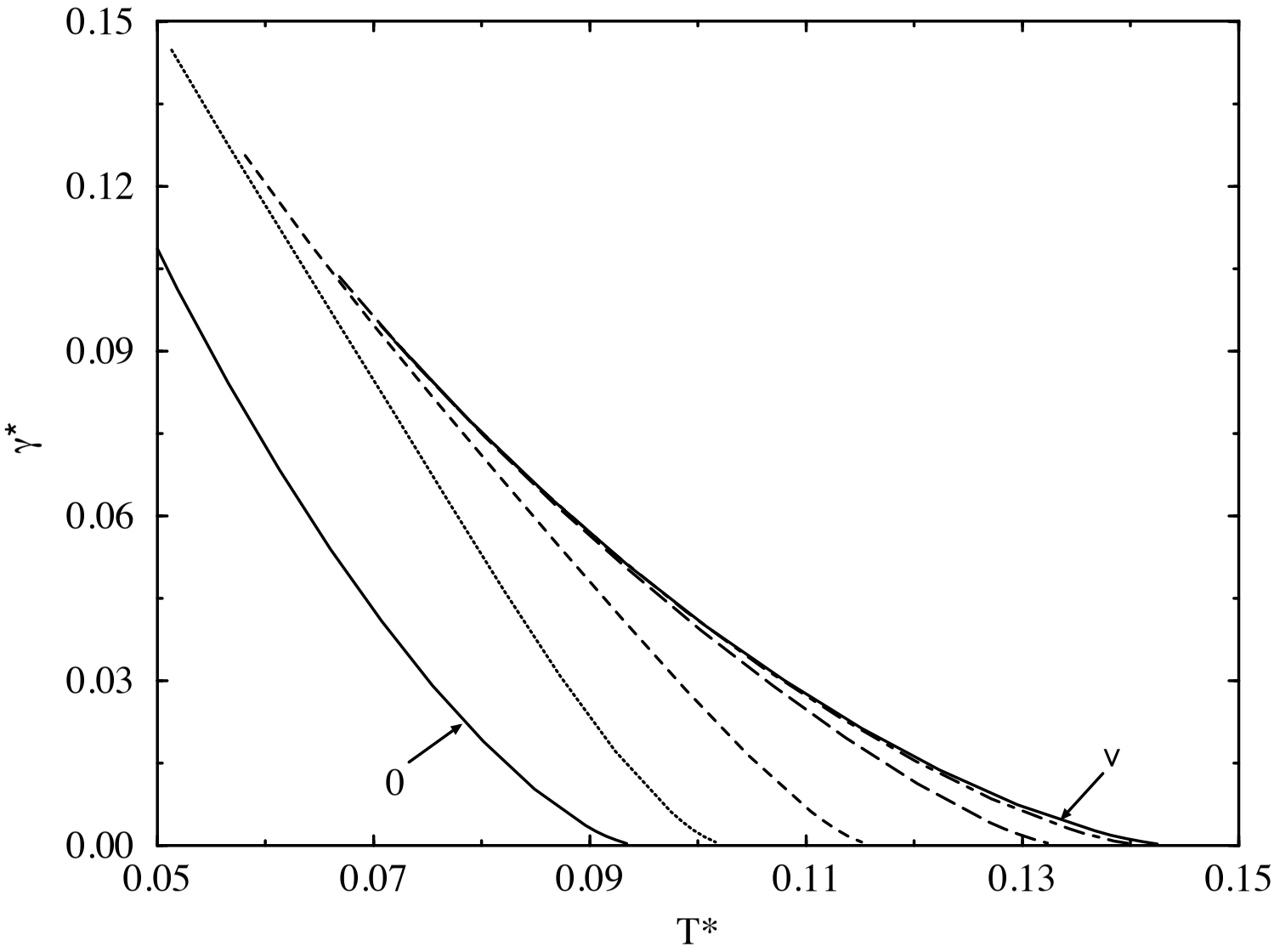
0.15
0.12
0.09
0.06
0.03
0.00
γ*
0.05
0.07
0.09
0.11
0.13
0.15
T*
0
V

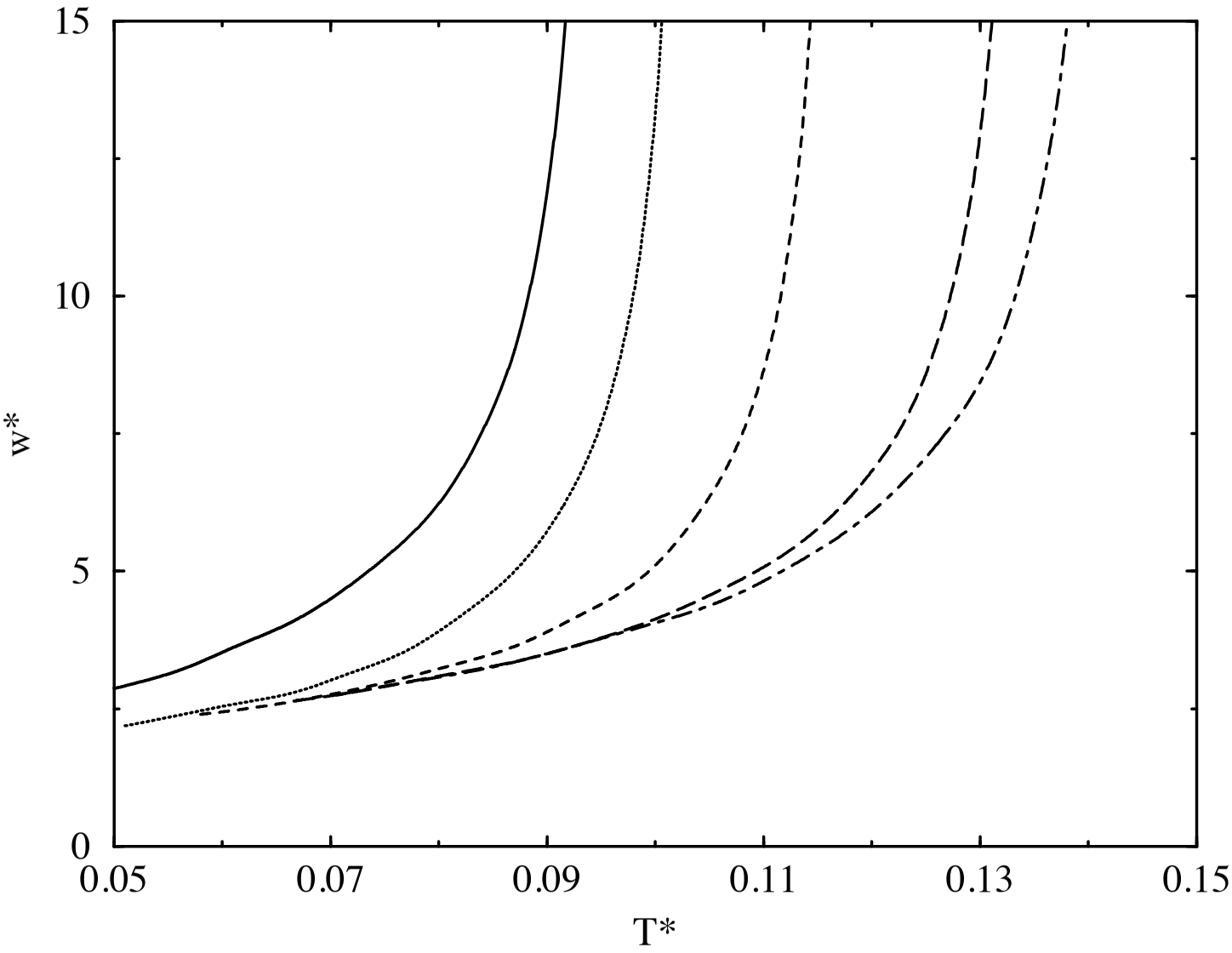
15
10
5
0
w*
0.05
0.07
0.09
0.11
0.13
0.15
T*

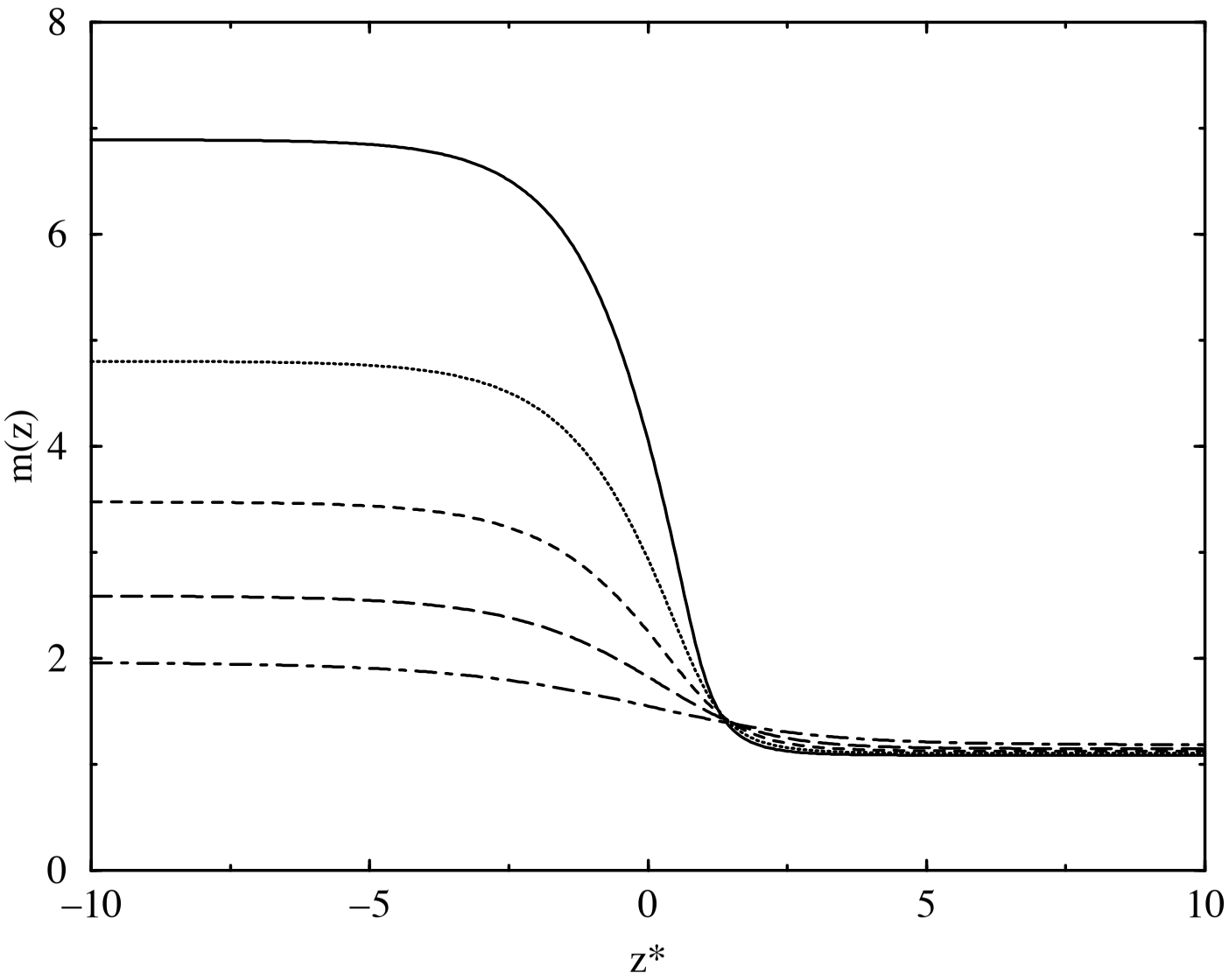
8
6
4
2
0
m(z)
–10
–5
0
5
10
z*

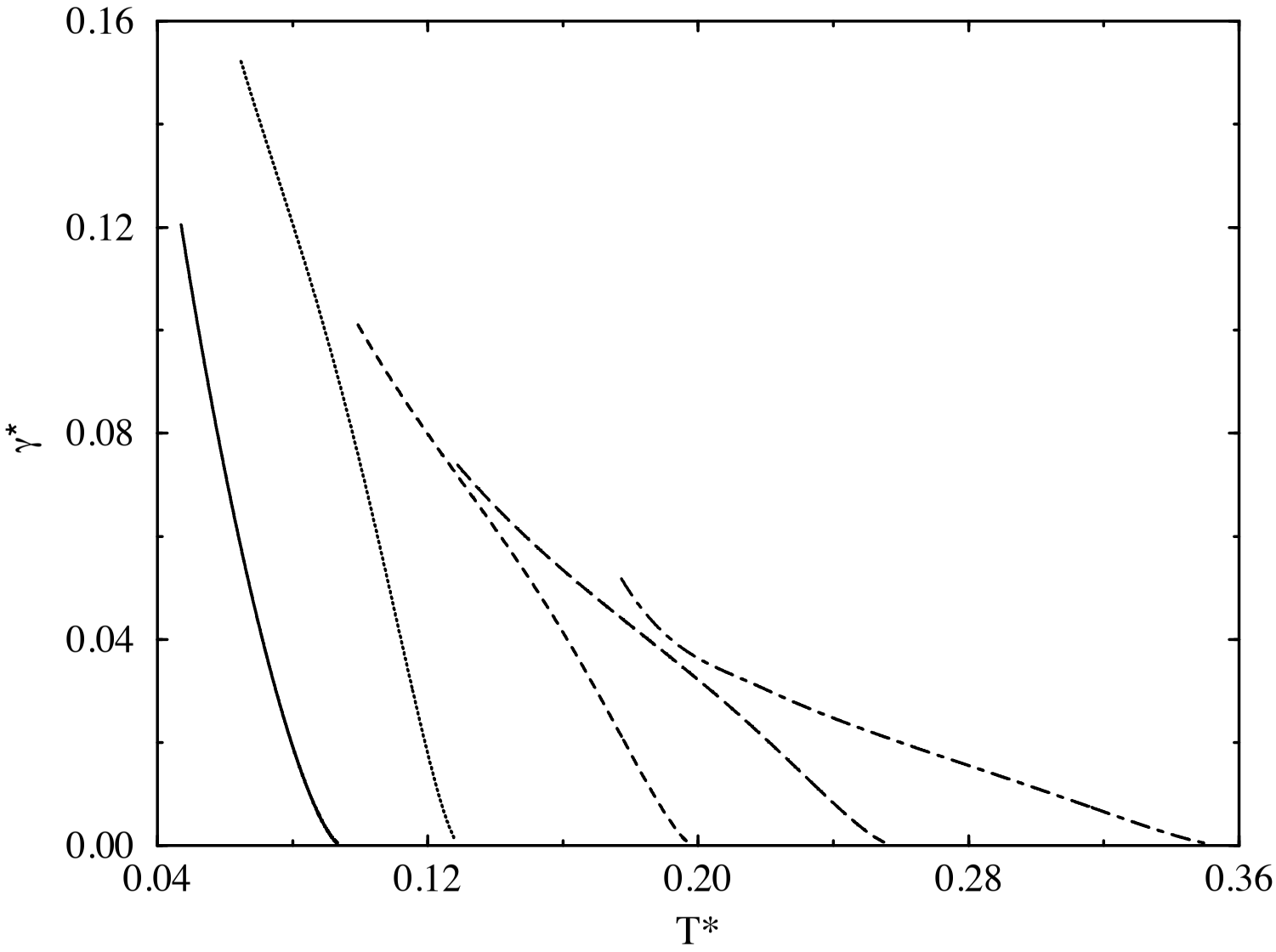
0.16
0.12
0.08
0.04
0.00
γ*
0.04
0.12
0.20
0.28
0.36
T*

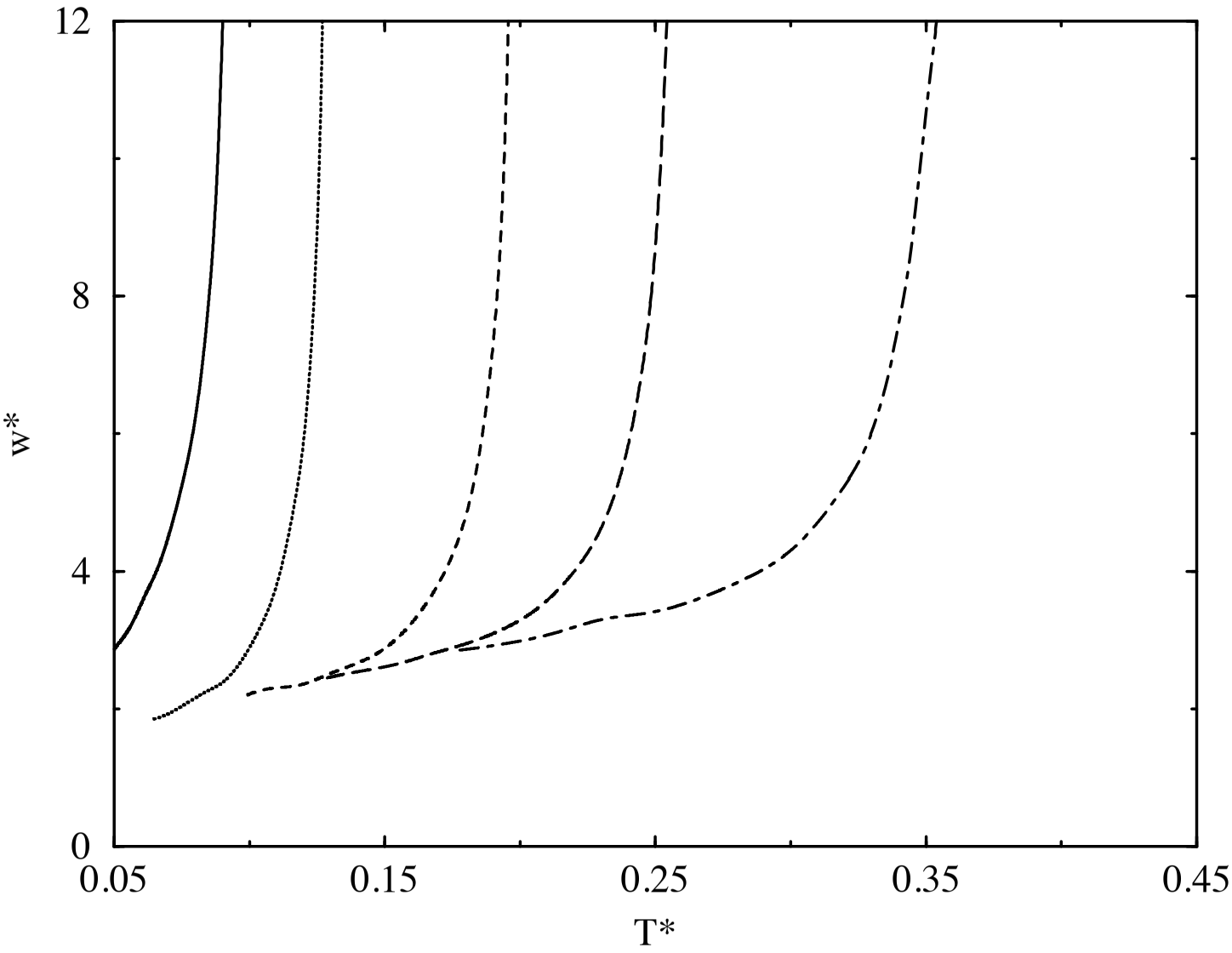
12
8
4
0
w*
0.05
0.15
0.25
0.35
0.45
T*

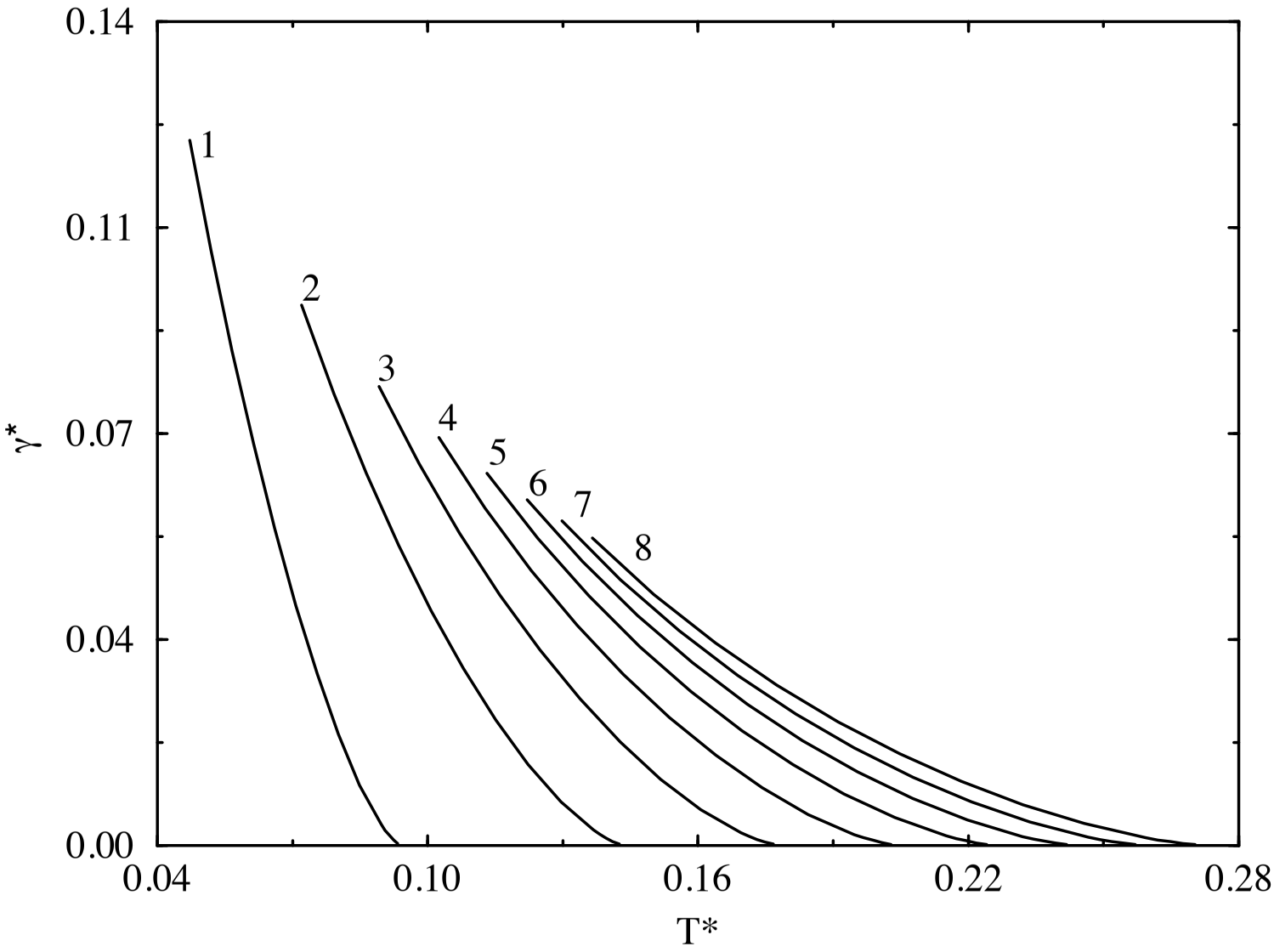
0.14
0.11
0.07
0.04
0.00
γ*
0.04
0.10
0.16
0.22
0.28
T*
1
2
3
4
5
6
7
8

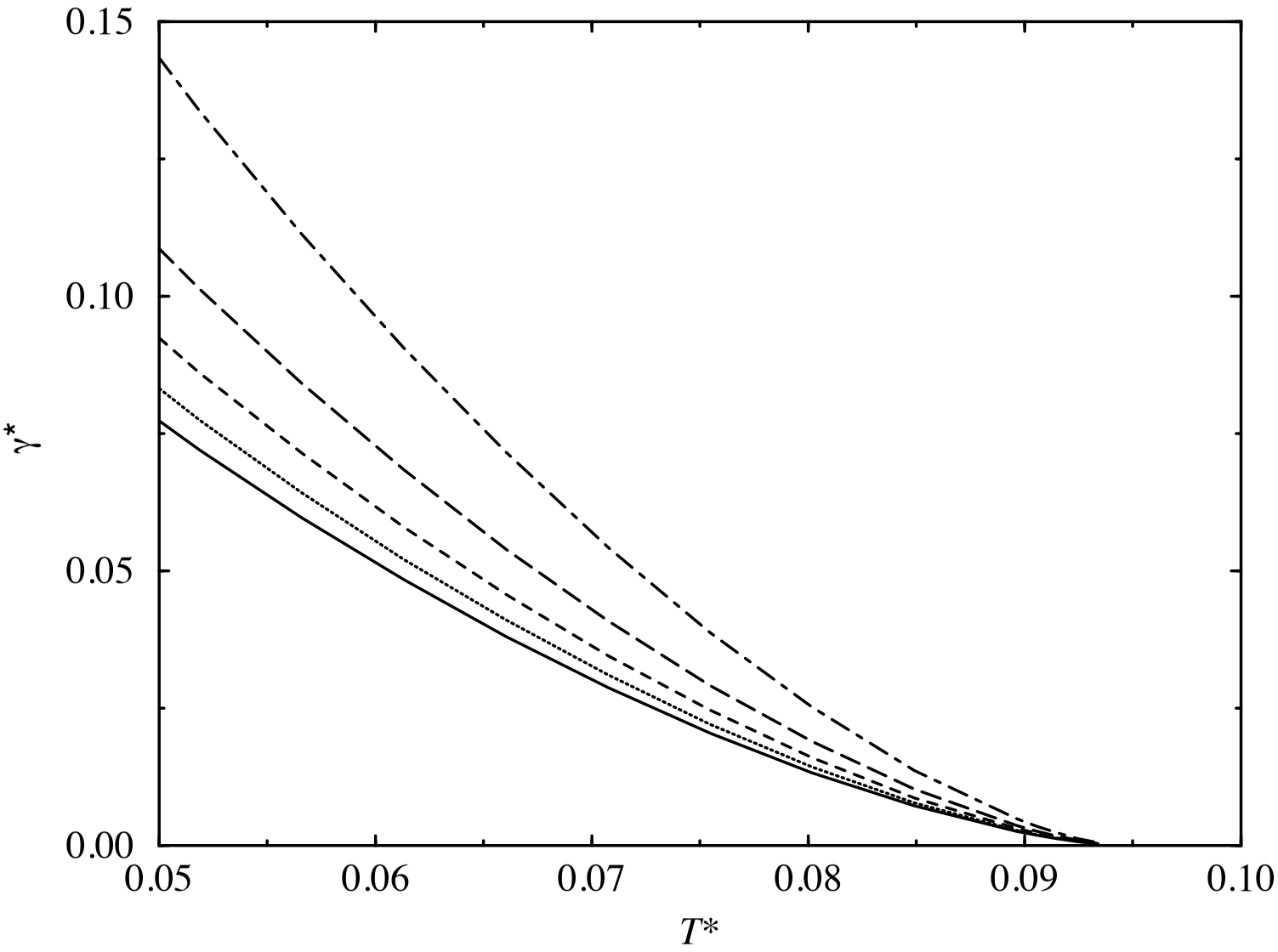
0.15
0.10
0.05
0.00
γ^*
0.05
0.06
0.07
0.08
0.09
0.10
T^*

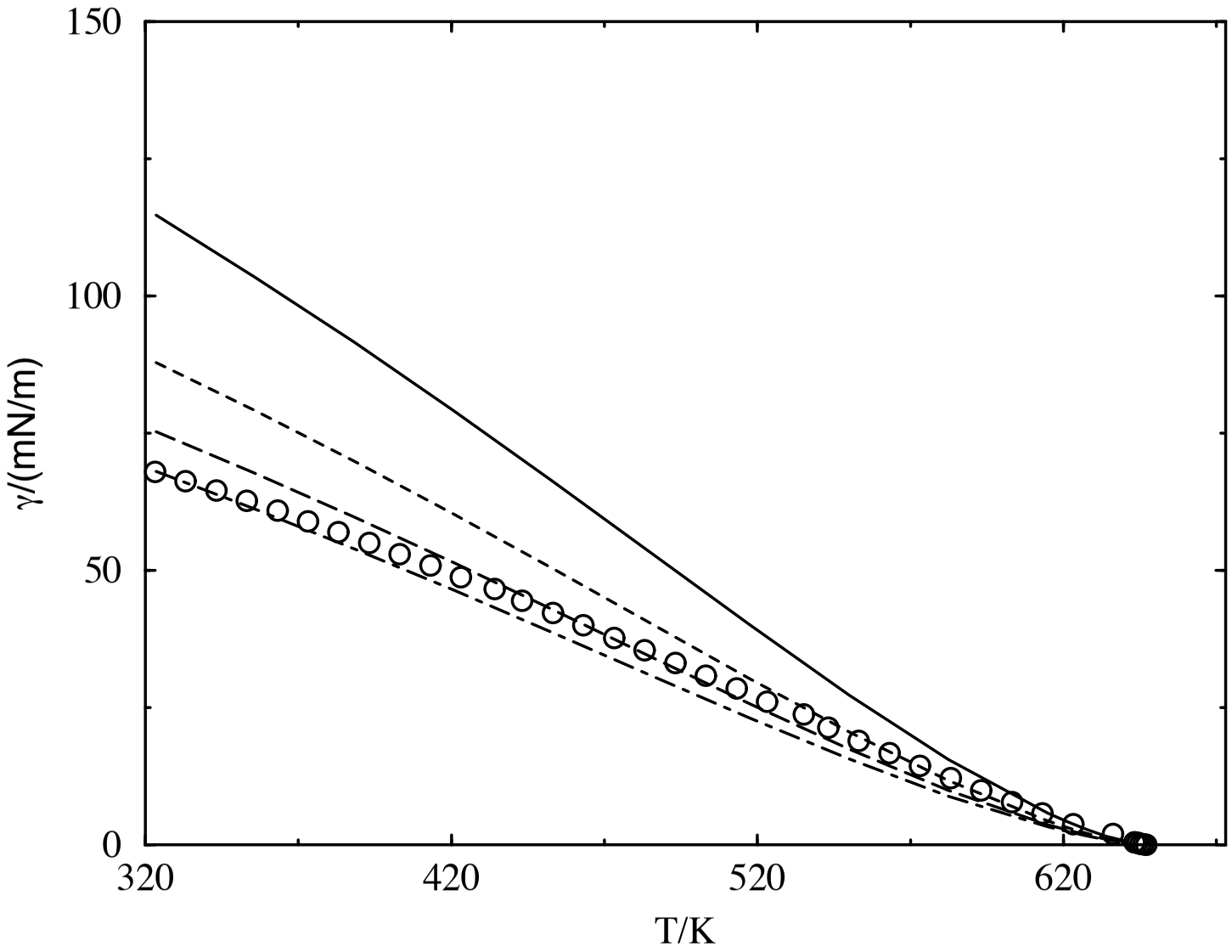
150
100
50
0
γ/(mN/m)
320
420
520
620
T/K

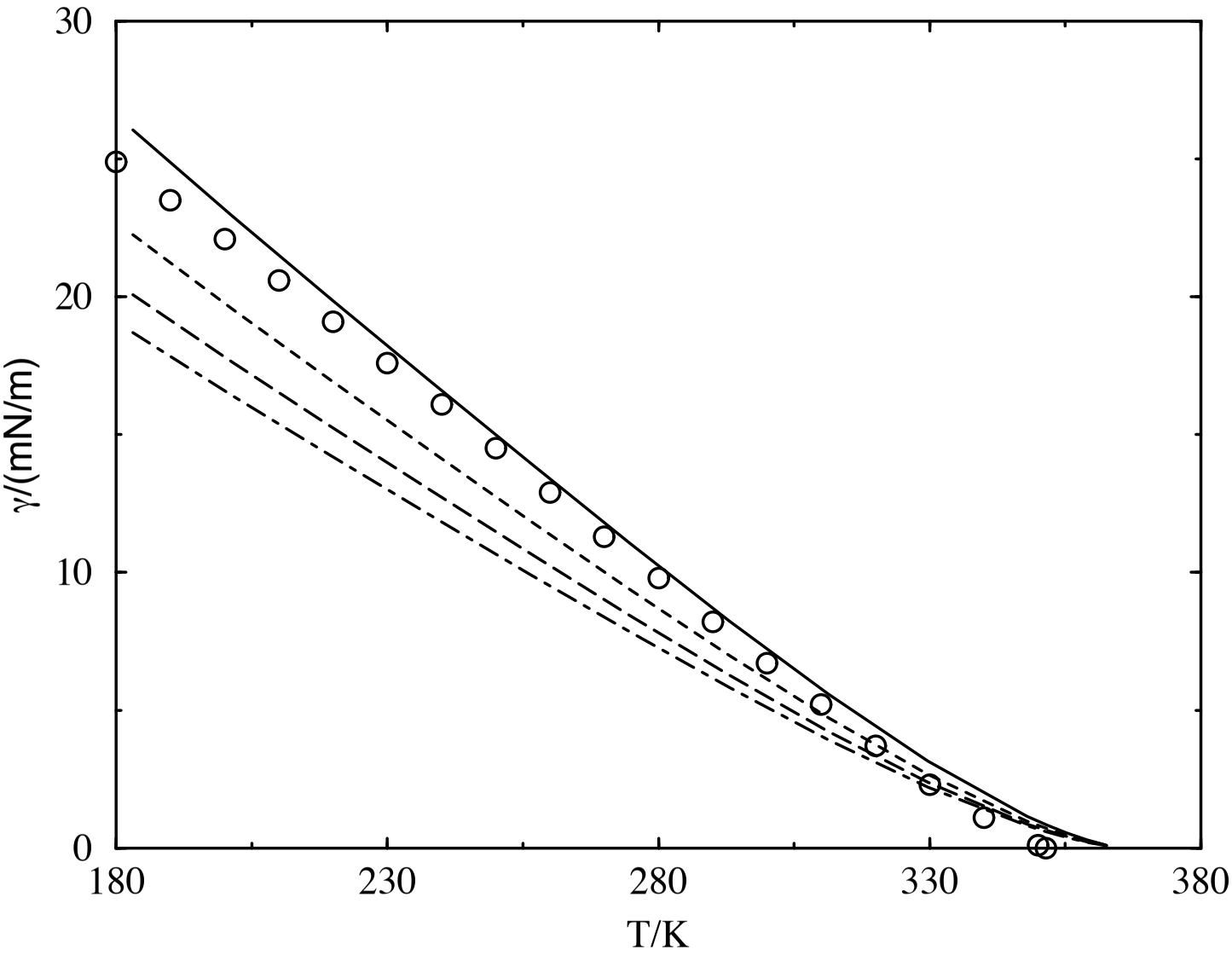
30
20
10
0
γ/(mN/m)
180
230
280
330
380
T/K

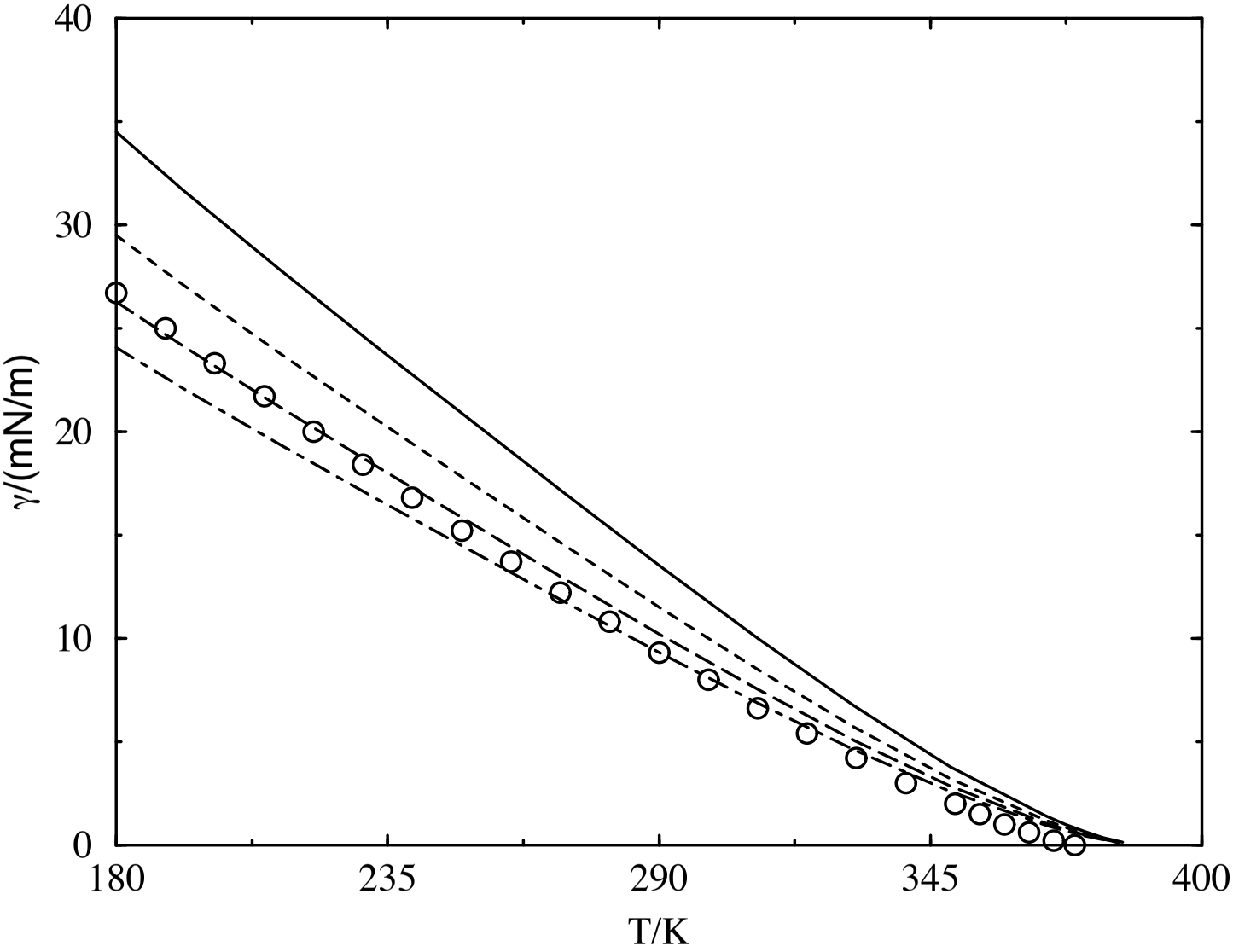
40
30
20
10
0
γ/(mN/m)
180
235
290
345
400
T/K